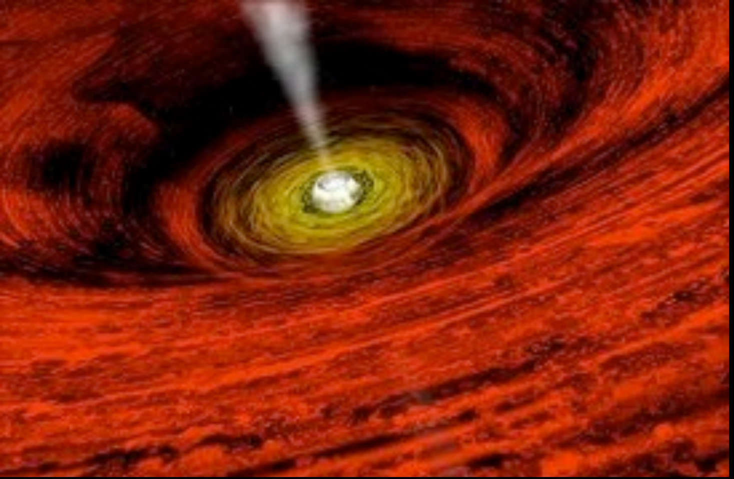

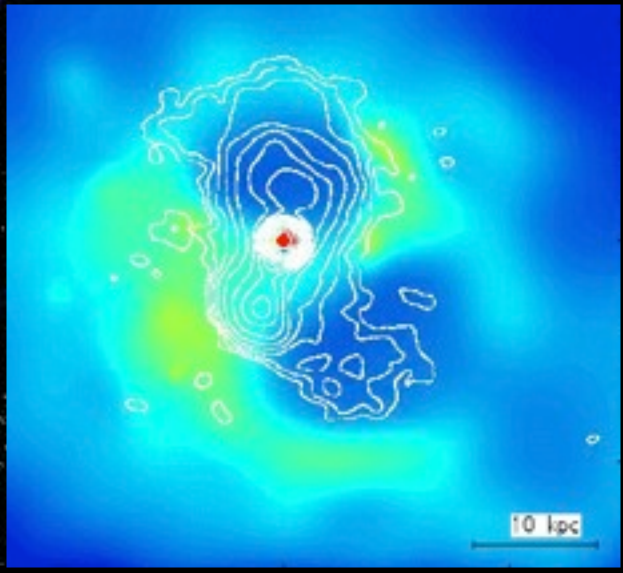

University of Waterloo
18 Sept 2013

Measuring All the Light Since the Big Bang with Gamma Rays

EBL Extragalactic Background Light

Joel Primack

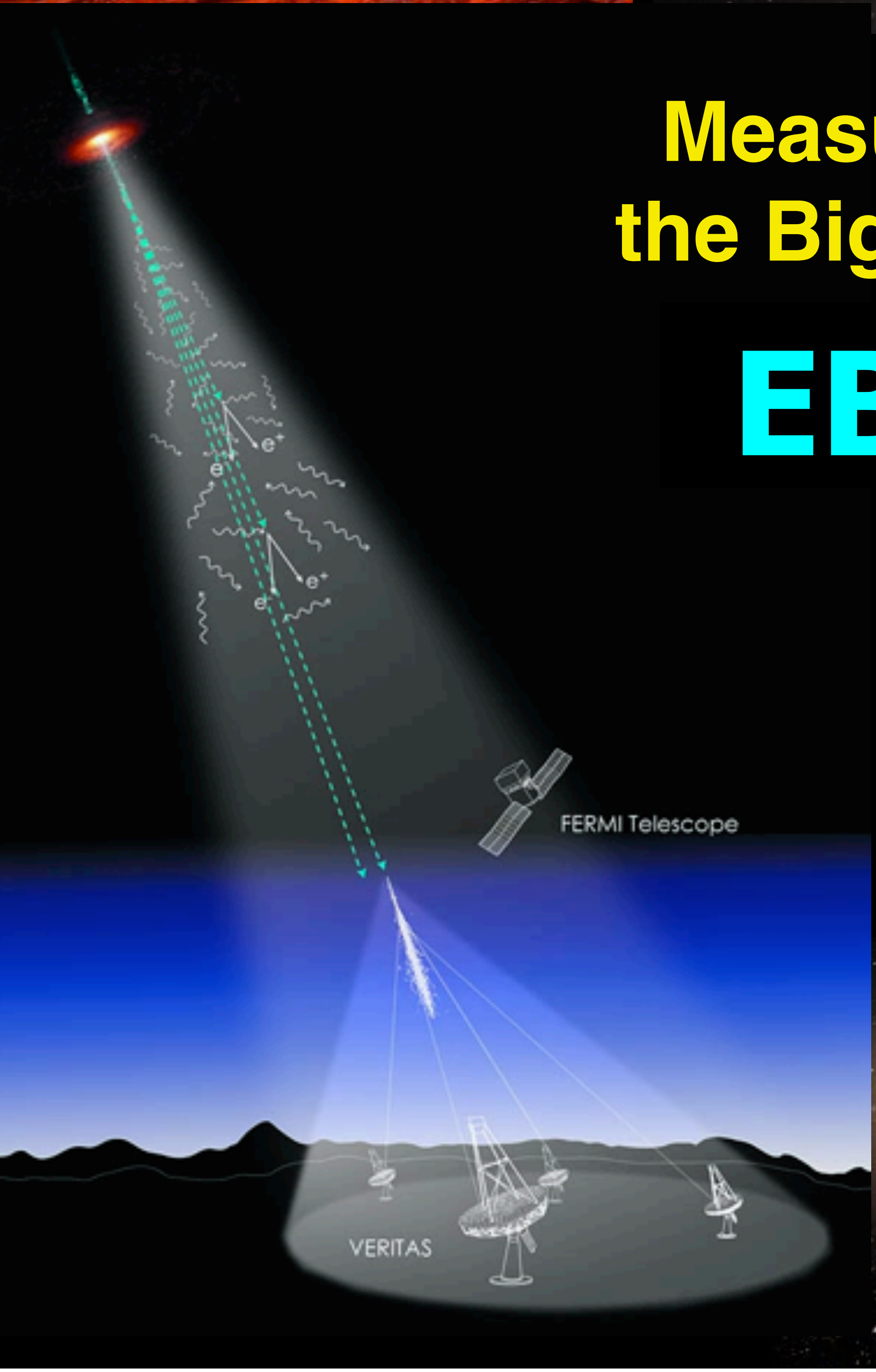

Extragalactic Background Light (EBL)

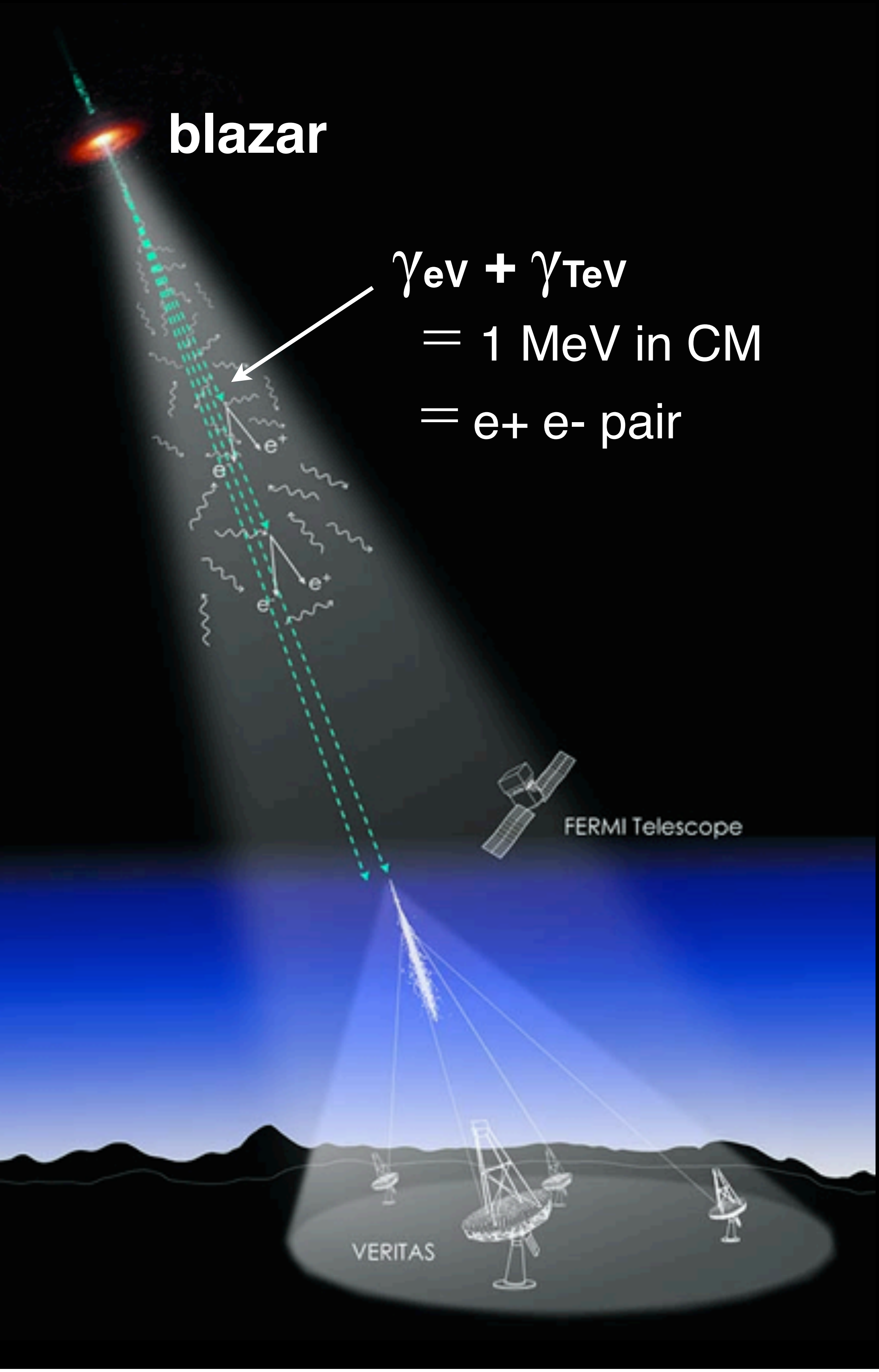

$\gamma_{eV} + \gamma_{TeV}$

$= 1$ MeV in CM

$=$ e+ e- pair

Data from (non-) attenuation of gamma rays from blazars and gamma ray bursts (GRBs) give upper limits on the EBL from the UV to the mid-IR that are only a little above the lower limits from observed galaxies. New data on attenuation of gamma rays from blazers now lead to statistically significant measurements of the cosmic gamma ray horizon (CGRH) as a function of source redshift and gamma ray energy that are independent of EBL models. These new measurements are consistent with recent EBL calculations based both on multiwavelength observations of thousands of galaxies and also on semi-analytic models of the evolving galaxy population. Such comparisons account for (almost) all the light, including that from galaxies too faint to see.

Cosmic Extragalactic Backgrounds

Herschel far-IR

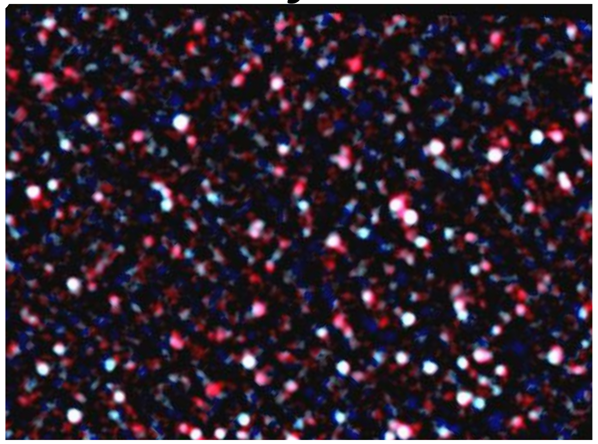

Spitzer mid-IR

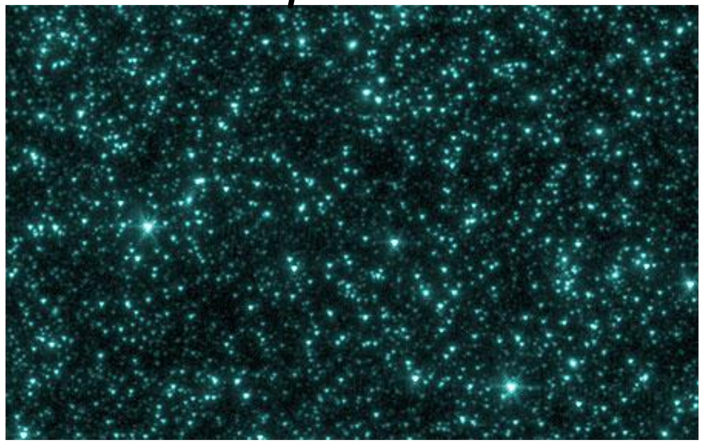

HST-optical/UV

0.850-1.2mm

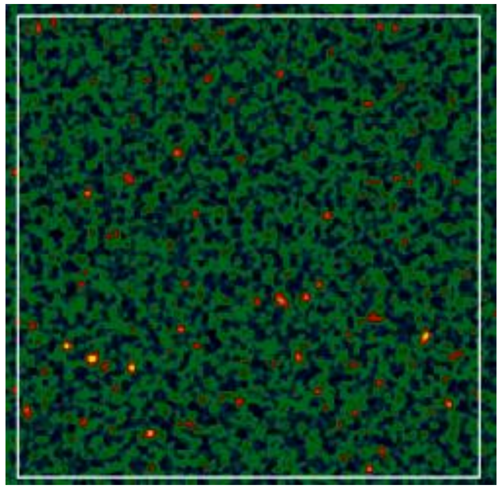

in the future:
ALMA, CCAT..

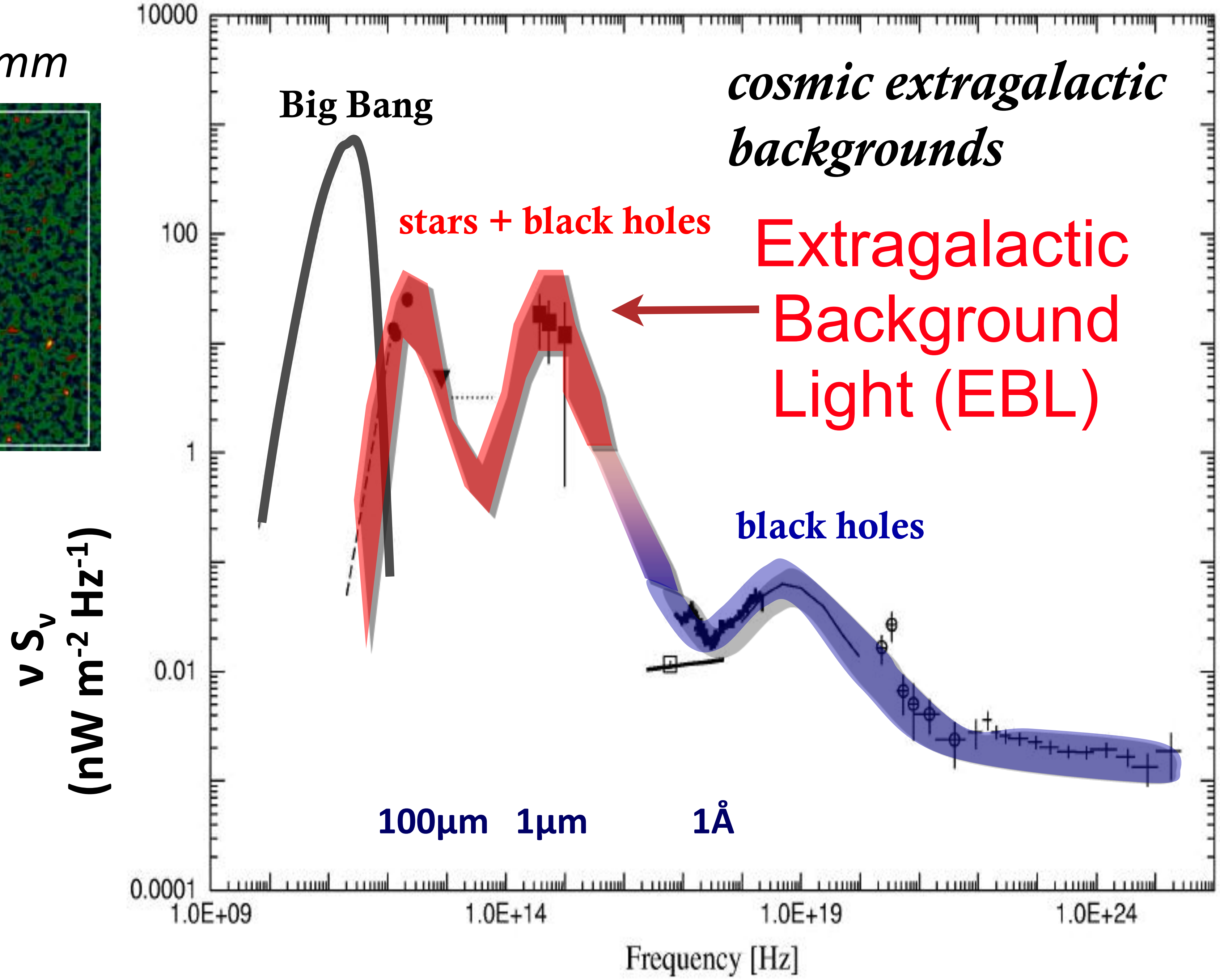

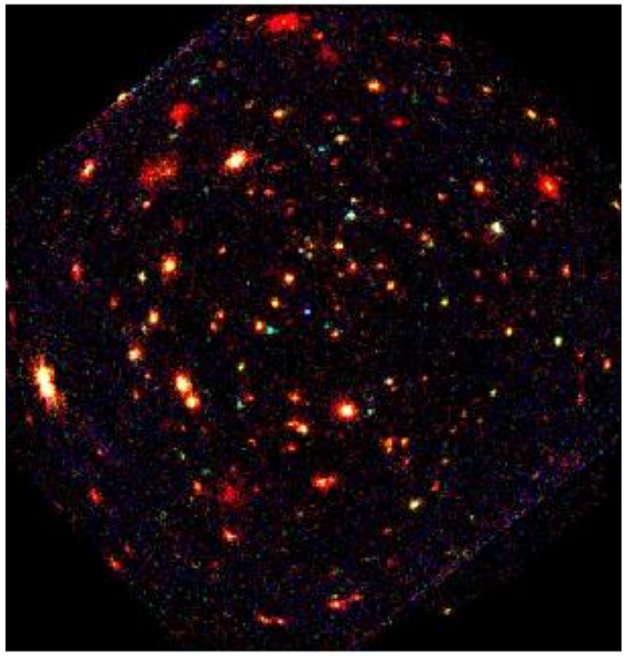

Chandra/XMM –X-ray

Extragalactic Background Light (EBL)

- The usual plot of λI_λ = dI/d log λ vs. log λ shows directly the

  ENERGY DENSITY $\rho_\lambda = (4\pi/c)\, \lambda I_\lambda$ in the EBL:

  $$1\ \mathrm{nW/m^2/sr} = 10^{-6}\ \mathrm{erg/s/cm^2/sr} = 2.6\times10^{-4}\ \mathrm{eV/cm^3}$$

  Total EBL $\Omega_{EBL}{}^{obs} = (4\pi/c)\, I_{EBL}/(\rho_{crit}\, c^2) = 2.0 \times10^{-4}\, I_{EBL}\, h_{70}{}^{-2}$

  The estimated $I_{EBL}{}^{obs}$= 60-100 nW/m^2/sr translates to

  $$\Omega_{EBL}{}^{obs} = (3\text{-}5) \times10^{-6} \quad (\text{about 5\% of } \Omega_{CMB})$$

- Local galaxies typically have $E_{FIR}/E_{opt} \approx 0.3$, while the EBL has E_{FIR}/E_{opt} = 1-2. **Hence most high-redshift radiation was emitted in the far IR.**

Luminosity-Dustiness Correlation

LIRG: $L_{FIR} \geq 10^{11} L_\odot$ ULIRG: $L_{FIR} \geq 10^{12} L_\odot$ HLIRG: $L_{FIR} \geq 10^{13} L_\odot$

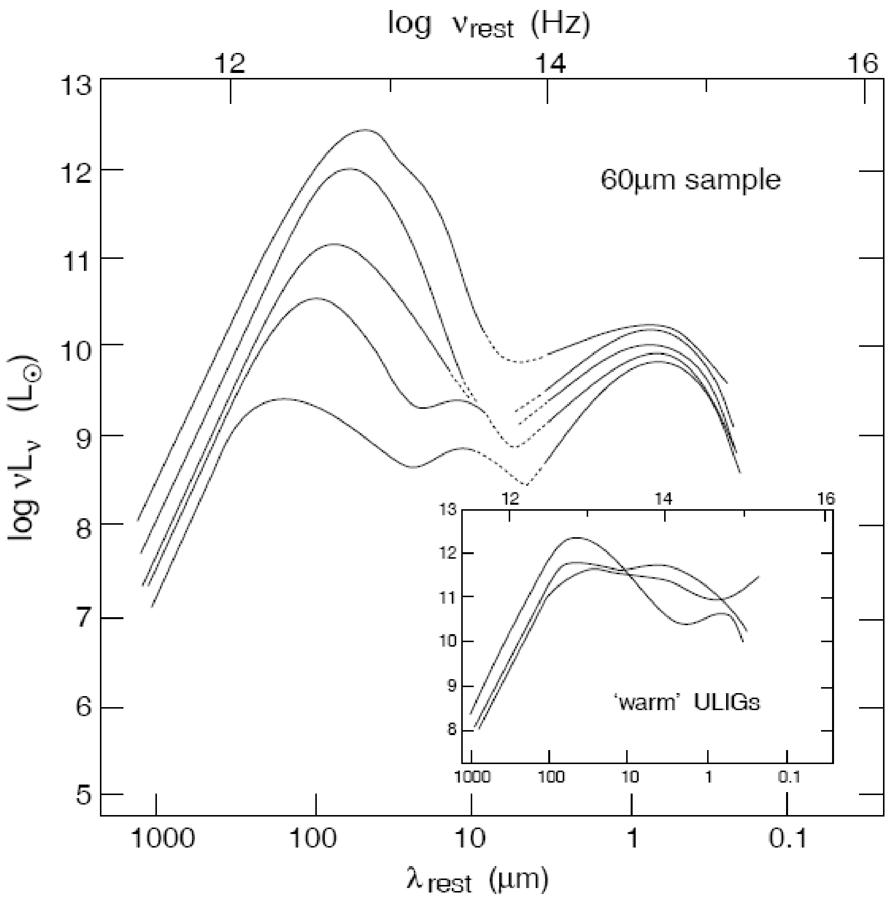

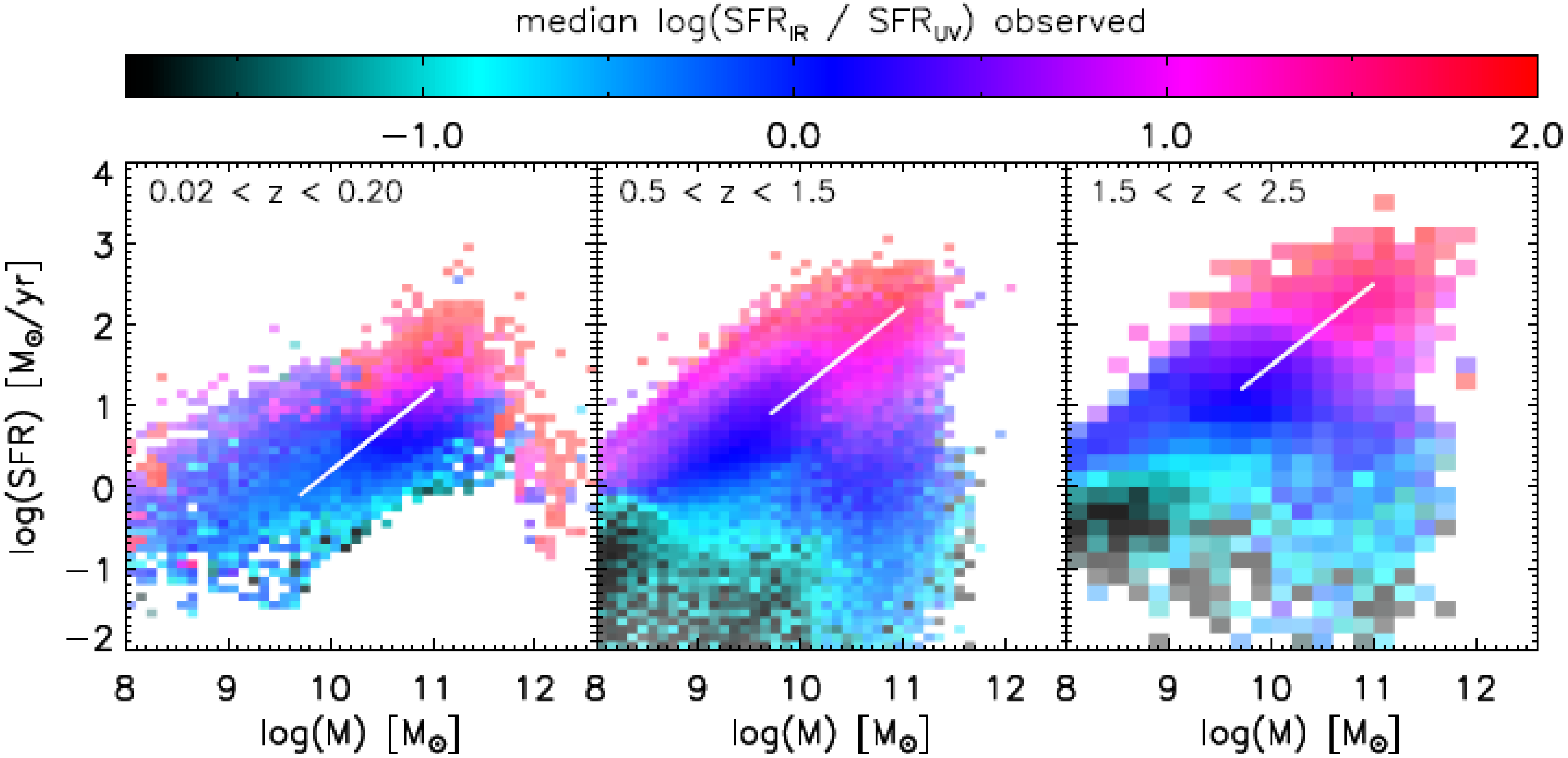

more luminous and massive galaxies are (much) more obscured: for starbursts and (U)LIRGs a de-reddening of the UV-emission does not succeed: the central starburst is behind a ‘black screen’ and the UV emission comes from a lower obscuration component; even de-reddened Hα fails by about a factor of 10; ULIRGs/starbursts often have ‘post-starburst’ UV/optical SEDs while the real starburst is completely hidden

Sanders & Mirabel 1996, Meurer et al. 1999,Wuyts et al. 2011

PILLAR OF STAR BIRTH
Carina Nebula in UV Visible Light

PILLAR OF STAR BIRTH
Carina Nebula in IR Light

Longer wavelength light penetrates the dust better

Longer wavelength gamma rays also penetrate the EBL better

Gamma Ray Attenuation due to $\gamma\gamma \rightarrow e^+e^-$

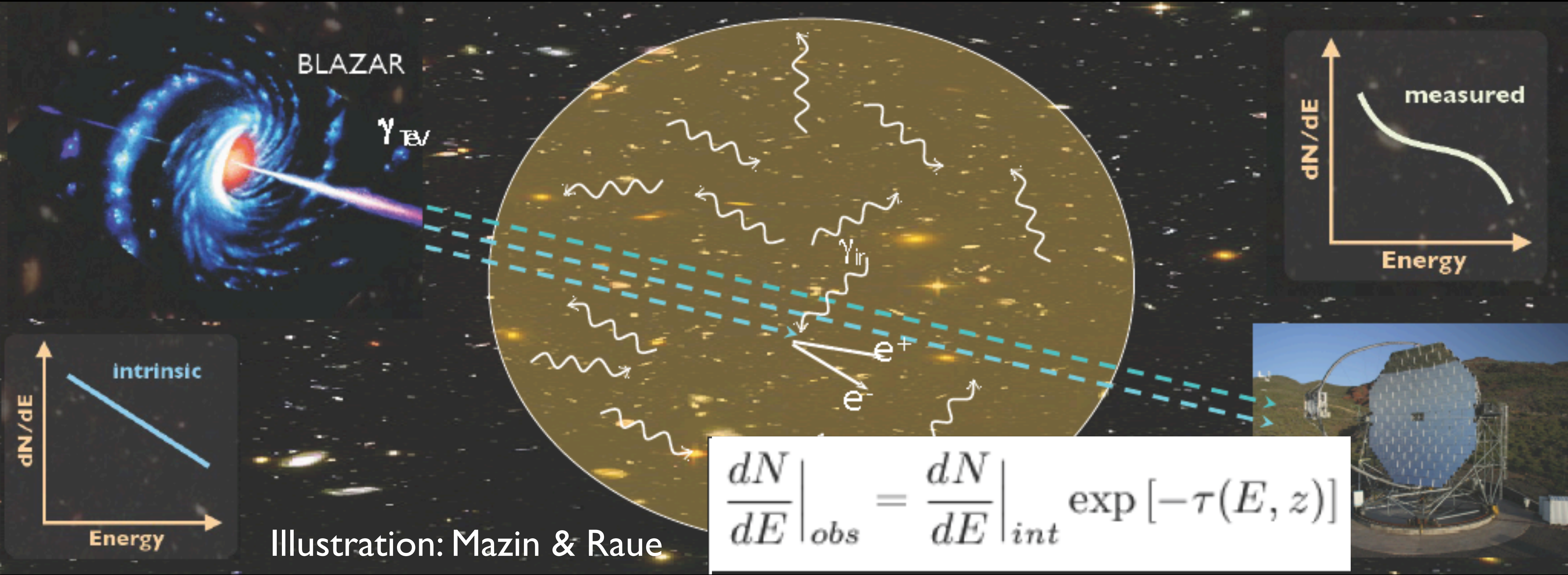

Illustration: Mazin & Raue

$$\left.\frac{dN}{dE}\right|_{obs} = \left.\frac{dN}{dE}\right|_{int} \exp\left[-\tau(E,z)\right]$$

If we know the intrinsic spectrum, we can infer the optical depth $\tau(E,z)$ from the observed spectrum. In practice, we typically *assume* that $dN/dE|_{int}$ is not harder than $E^{-\Gamma}$ with $\Gamma = 1.5$, since local sources have $\Gamma \geq 2$. More conservatively, we can assume that $\Gamma \geq 2/3$.

Local EBL Observations

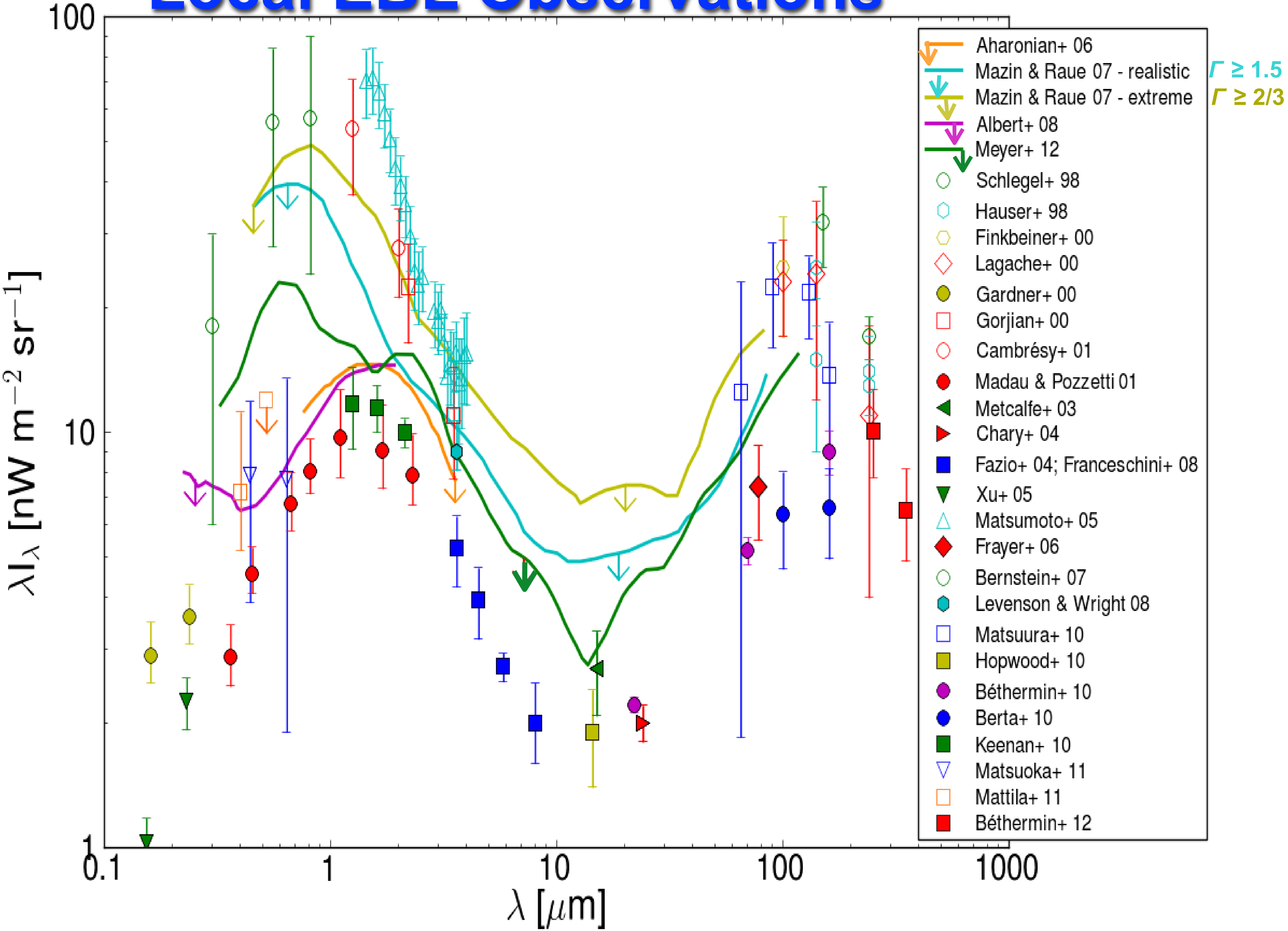

EBL Evolution Calculated from Observations Using AEGIS Multiwavelength Data

Alberto DomÍnguez, Joel Primack, et al. (MNRAS, 2011)

$$j_i(\lambda, z) = j_i^{faint} + j_i^{mid} + j_i^{bright} =$$

$$= \int_{M_1}^{M_2} \underline{\Phi(M_K, z)}\,\underline{f_i}\,\underline{T_i(M_K, \lambda)}\,dM_K +$$

$$+ \int_{M_2}^{M_3} \underline{\Phi(M_K, z)}\,\underline{m_i}\,\underline{T_i(M_K, \lambda)}\,dM_K +$$

$$+ \int_{M_3}^{M_4} \underline{\Phi(M_K, z)}\,\underline{b_i}\,\underline{T_i(M_K, \lambda)}\,dM_K$$

Spectral energy distributions
SWIRE template library, Polletta+ 07

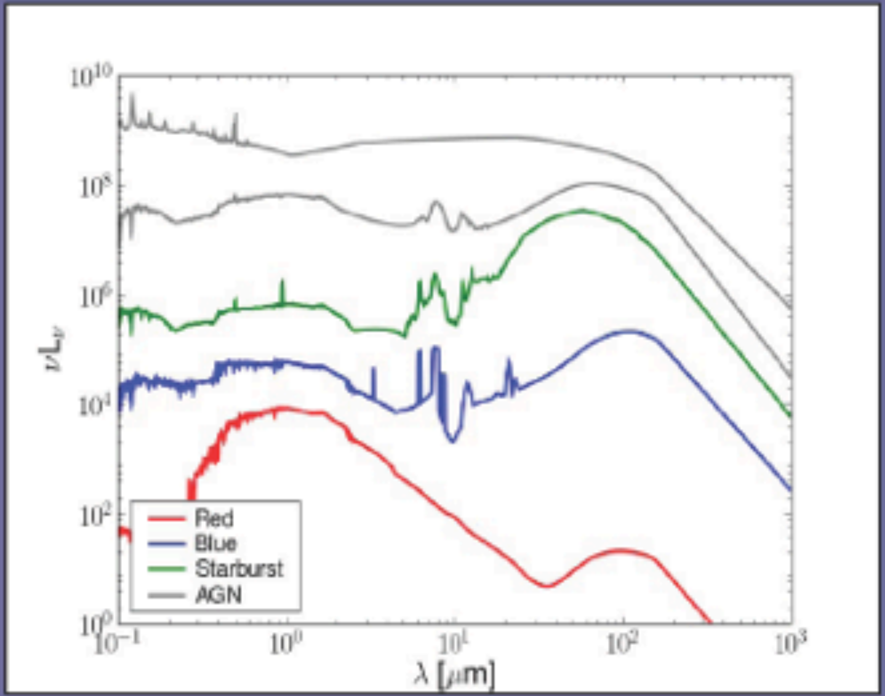

Luminosity function
observed K-band, Cirasuolo+ 09

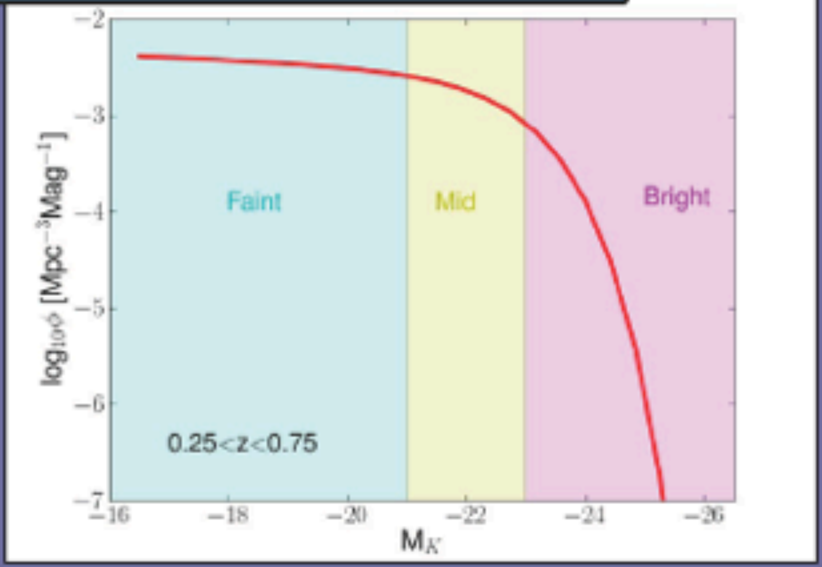

Spectral-type fractions

$$\lambda I_\lambda(z) = \frac{c}{4\pi} \int_z^{z_{max}} j_{total}[\lambda(1+z)/(1+z'), z'] \left|\frac{dt}{dz'}\right| dz'$$

0.7 □°

The AEGIS Survey...

...is unlocking the secrets of galaxy and large-scale structure formation over the last 9 billion years.

AEGIS is targeted on a special area of the sky, called the Extended Groth Strip (EGS), that has been observed with the world's most powerful telescopes on the ground and in space, from X-rays to radio waves.

Each telescope contributes its own key information to create a complete portrait of every galaxy. By looking out far into space and back in time, AEGIS literally shows us galaxies in all their glory that are emerging from infancy into adulthood. More...

http://aegis.ucolick.org/

χ^2 SED Fitting

Le PHARE code for fitting the SWIRE templates in FUV, NUV, B, R, I, Ks, IRAC1, 2, 3, 4 and MIPS24

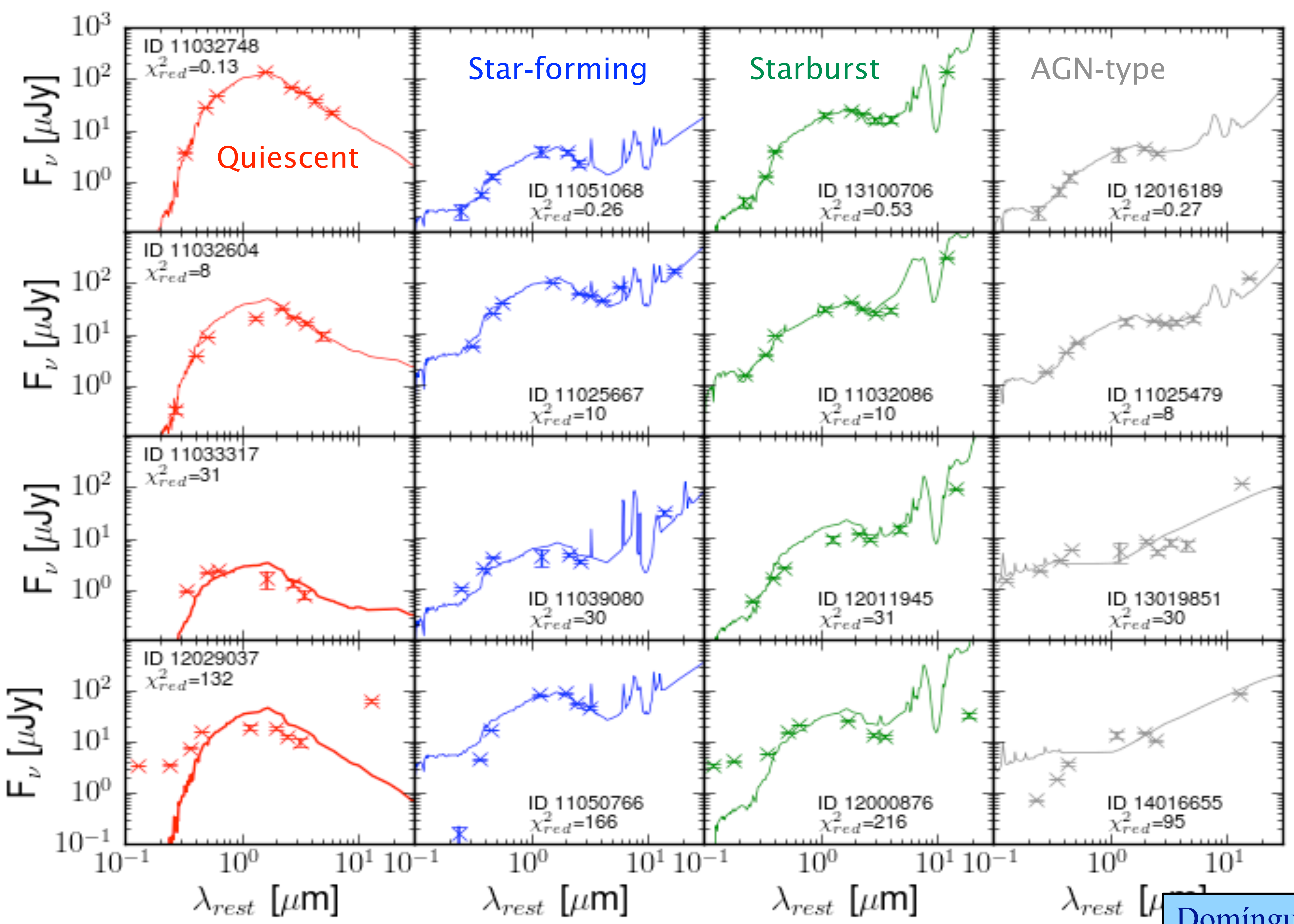

Best SED Fits

Worst SED Fits

Domínguez+ 11

SED-Type Evolution

Local fractions, z<0.2:

Goto+ 03, morphologically classified from Sloan converted to spectral classification using results from Galaxy Zoo

Skibba+ 09 ~6% blue ellipticals

Schawinski+ 09 ~25% red spirals

Results:

35% red-type galaxies
65% blue-type galaxies

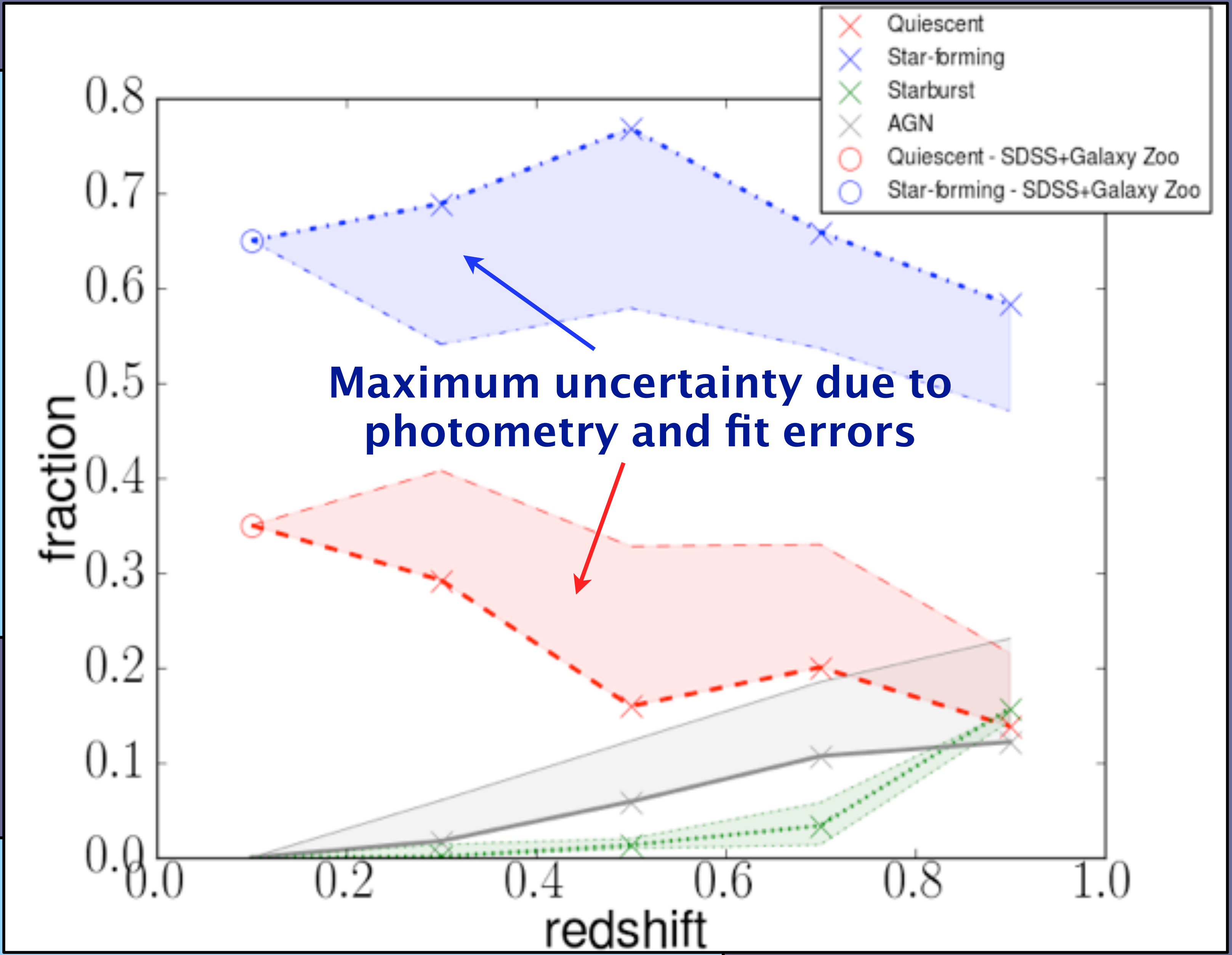

Maximum uncertainty due to photometry and fit errors

High-redshift universe, z>1:

Two approaches:
1. Keep constant the fractions of our last redshift bin (Fiducial Model), or
2. Quickly increase starburst population from 16% at z = 0.9 to 60% at z ≥ 2

We find that the differences in the predicted EBL are small except at long wavelengths, affecting attenuation only for E ≥ 5 TeV.

Domínguez+11

Local Luminosity Density

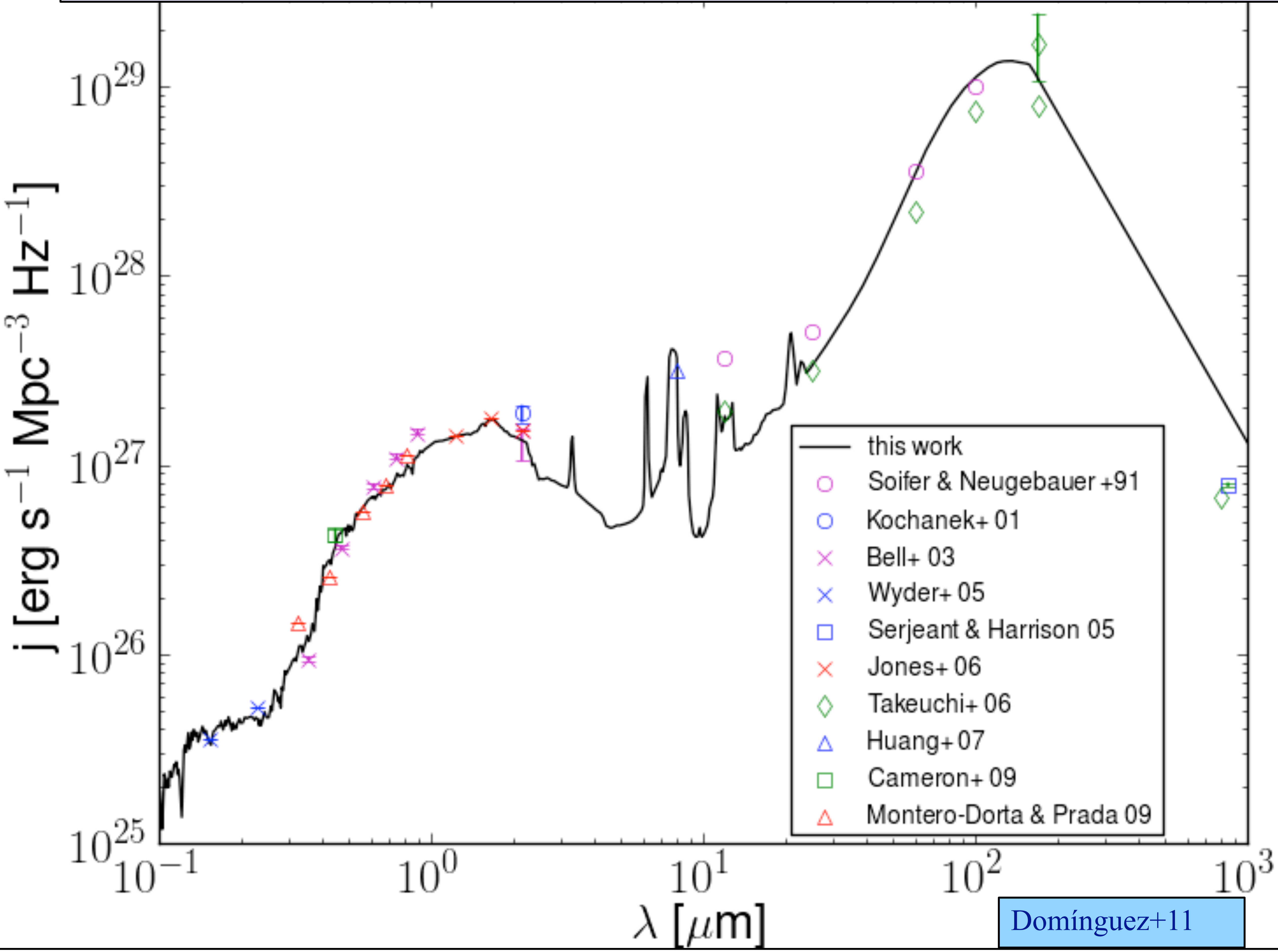

Domínguez+11

Local EBL Observations

vs. Domínguez+11

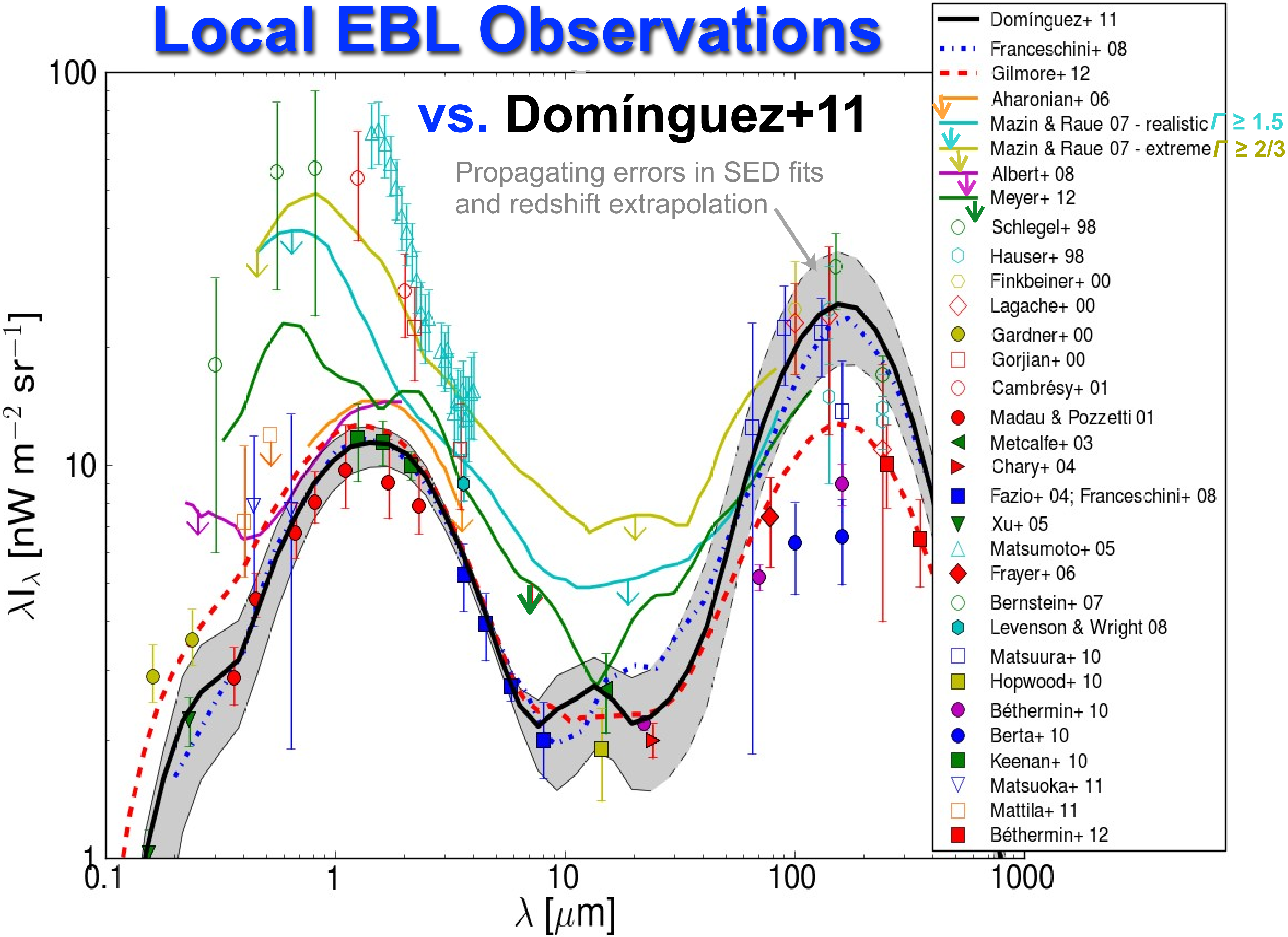
Propagating errors in SED fits and redshift extrapolation

EBL Calculated by Forward Evolution using SAMs

When we first tried doing this (Primack & MacMinn 1996, presented at Felix Aharonian's first Heidelberg conference), both the stellar initial mass function (IMF) and the values of the cosmological parameters were quite uncertain. After 1998, the cosmological model was known to be ΛCDM although it was still necessary to consider various cosmological parameters in models. Now the parameters are known rather precisely, and our latest semi-analytic model (**SAM**) used the current (WMAP5/7/9) cosmological parameters. With improved simulations and better galaxy data, we can now normalize SAMs better and determine the key astrophysical processes to include in them.

Remaining uncertainties include whether the IMF is different in different galaxies (possibly "bottom-heavy" in massive galaxies), feedback from AGN, the nature of sub-mm galaxies, and the star formation rate at high redshifts.

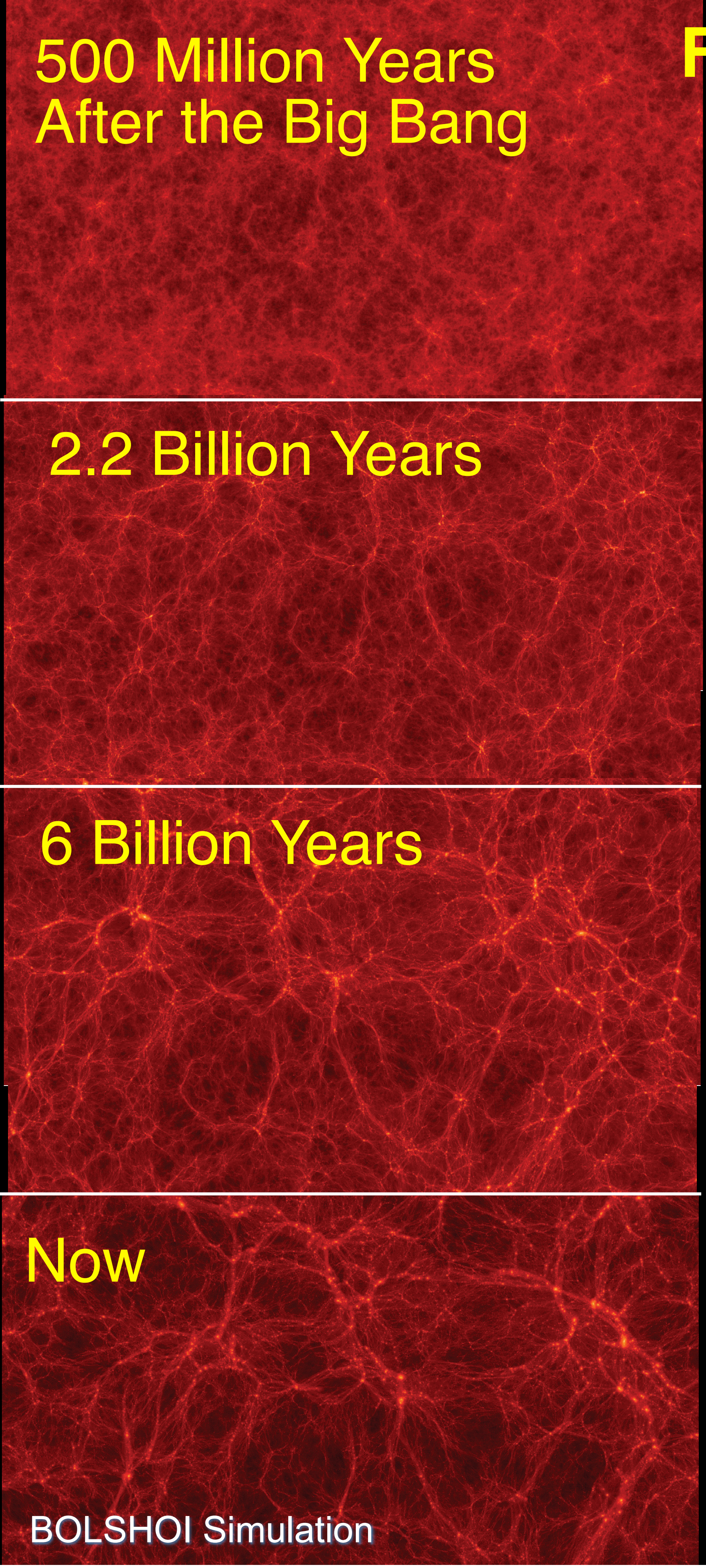

BOLSHOI Simulation

Forward Evolution

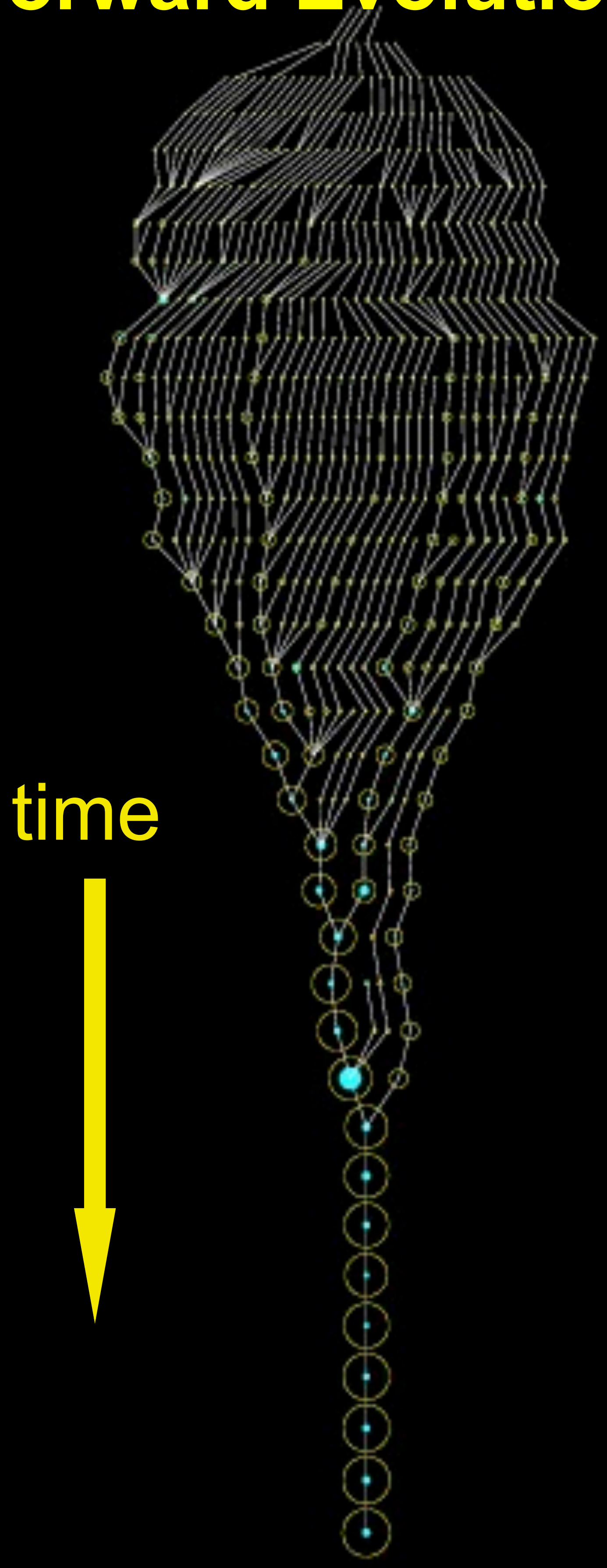

Wechsler et al. 2002

Present status of ΛCDM “Double Dark” theory:

- cosmological parameters are now well constrained by observations

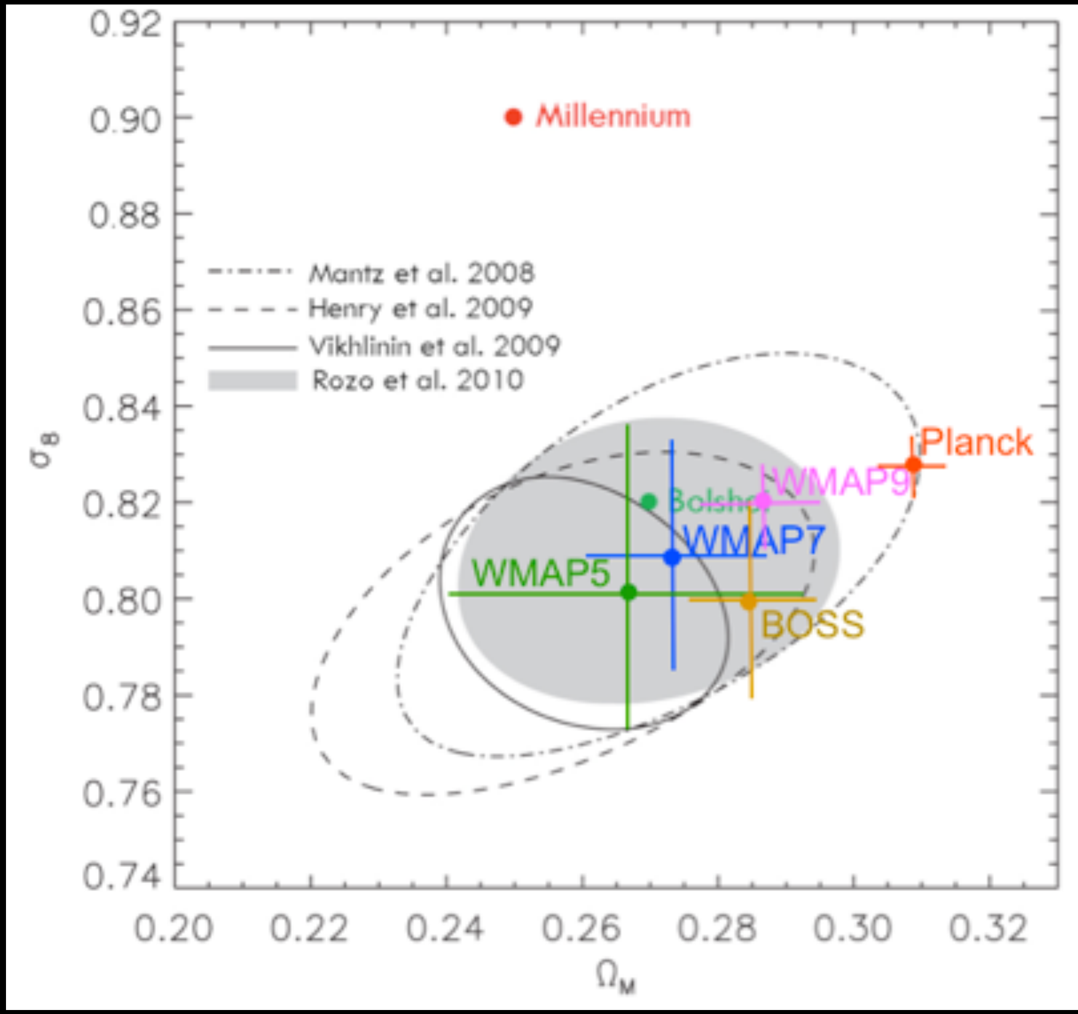

- mass accretion history of dark matter halos is represented by ‘merger trees’ like the one at left

Determination of σ_8 and Ω_M from CMB+

WMAP+SN+Clusters Planck+WP+HighL+BAO

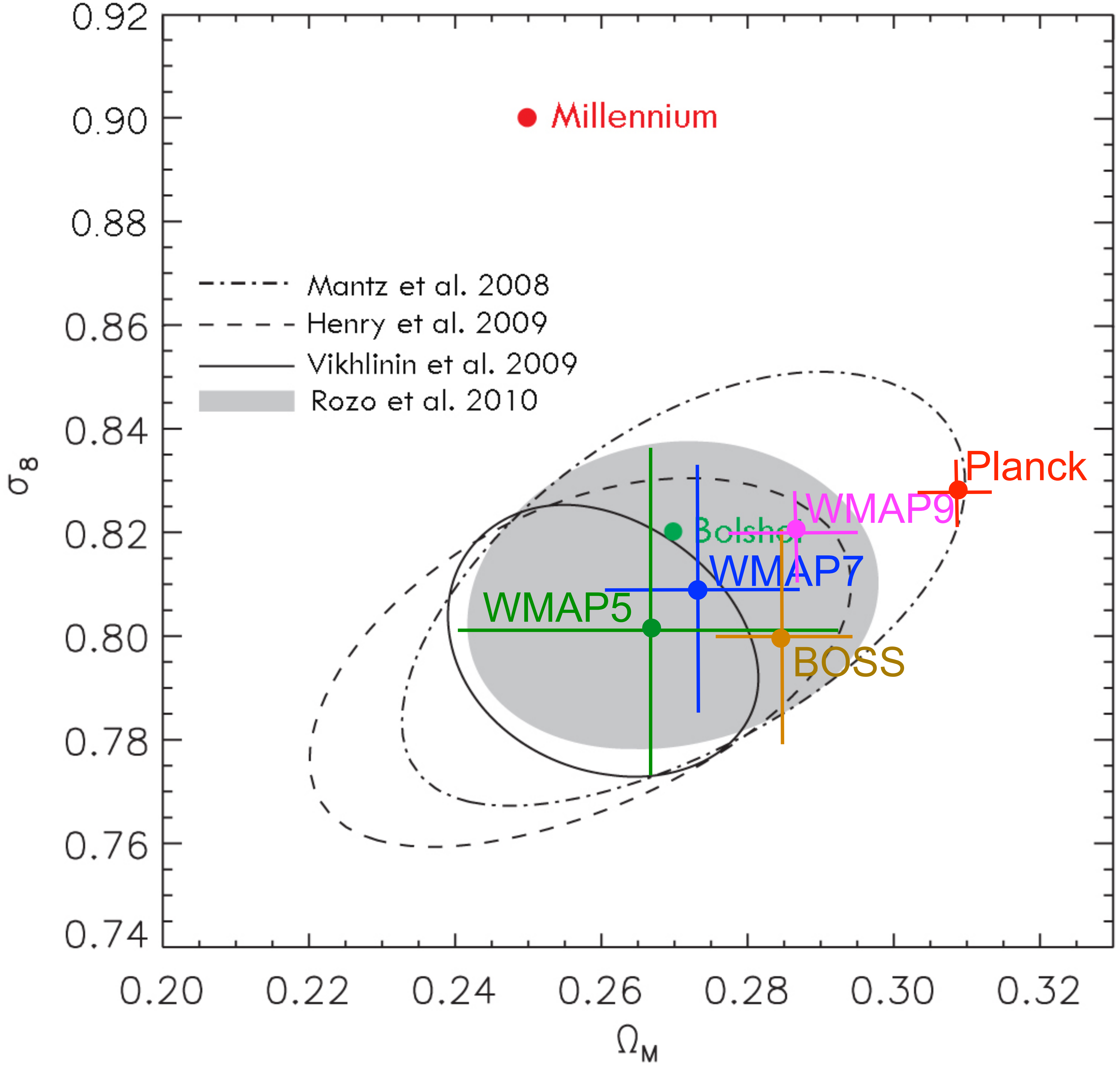

Galaxy Formation in ΛCDM

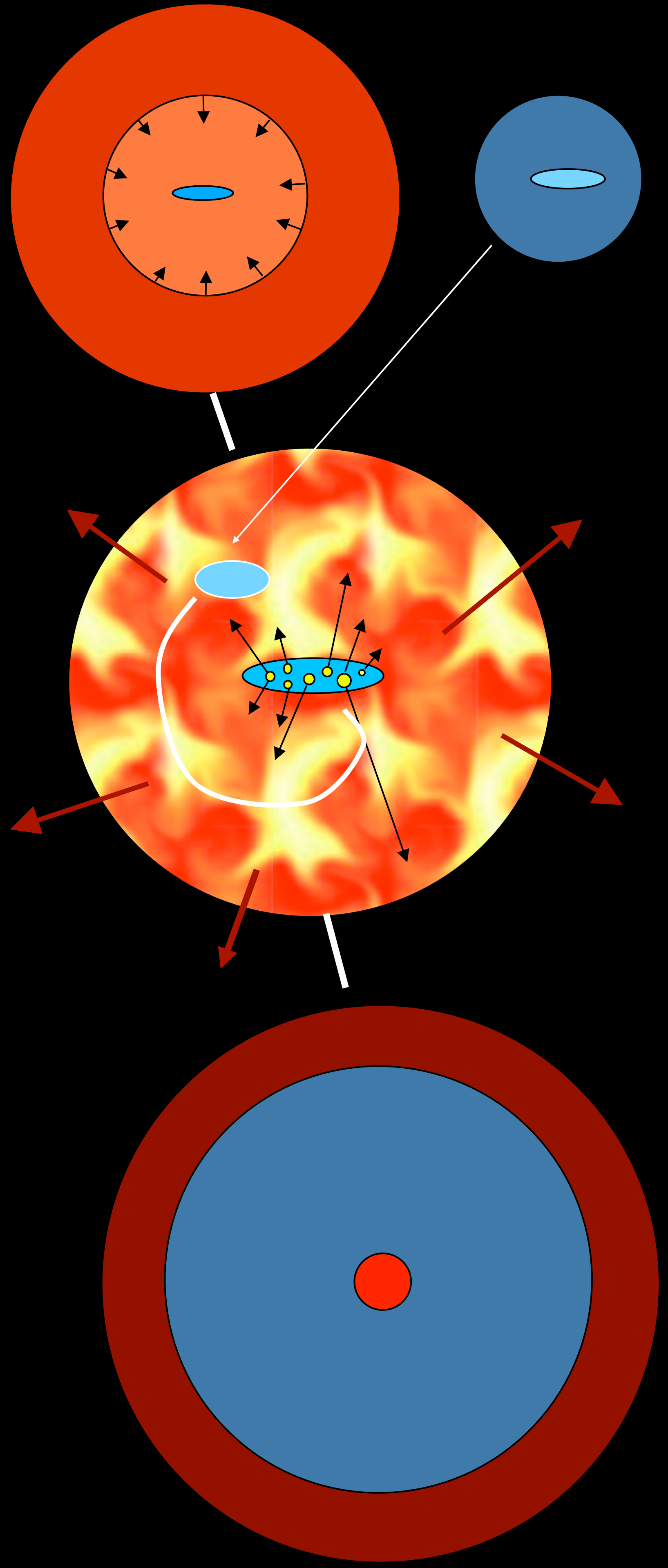

- gas is collisionally heated when perturbations ‘turn around’ and collapse to form gravitationally bound structures
- gas in halos cools via atomic line transitions (depends on density, temperature, and metallicity)
- cooled gas collapses to form a rotationally supported disk
- cold gas forms stars, with efficiency a function of gas density (e.g. Schmidt-Kennicutt Law)
- massive stars and SNae reheat (and in small halos expel) cold gas and some metals
- galaxy mergers trigger bursts of star formation; ‘major’ mergers transform disks into spheroids and fuel AGN
- AGN feedback cuts off star formation

White & Frenk 1991; Kauffmann+1993; Cole+94; Somerville & Primack 99; Cole+00; Somerville, Primack, & Faber 01; Croton et al. 2006; Somerville +08; Fanidakis+09; Guo+2011; Somerville, Gilmore, Primack, & Domínguez 2012 & Gilmore +2012 (discussed here); Porter, Somerville, Primack 2013abc

Some Results from our Semi-Analytic Models

z=0 Luminosity Density

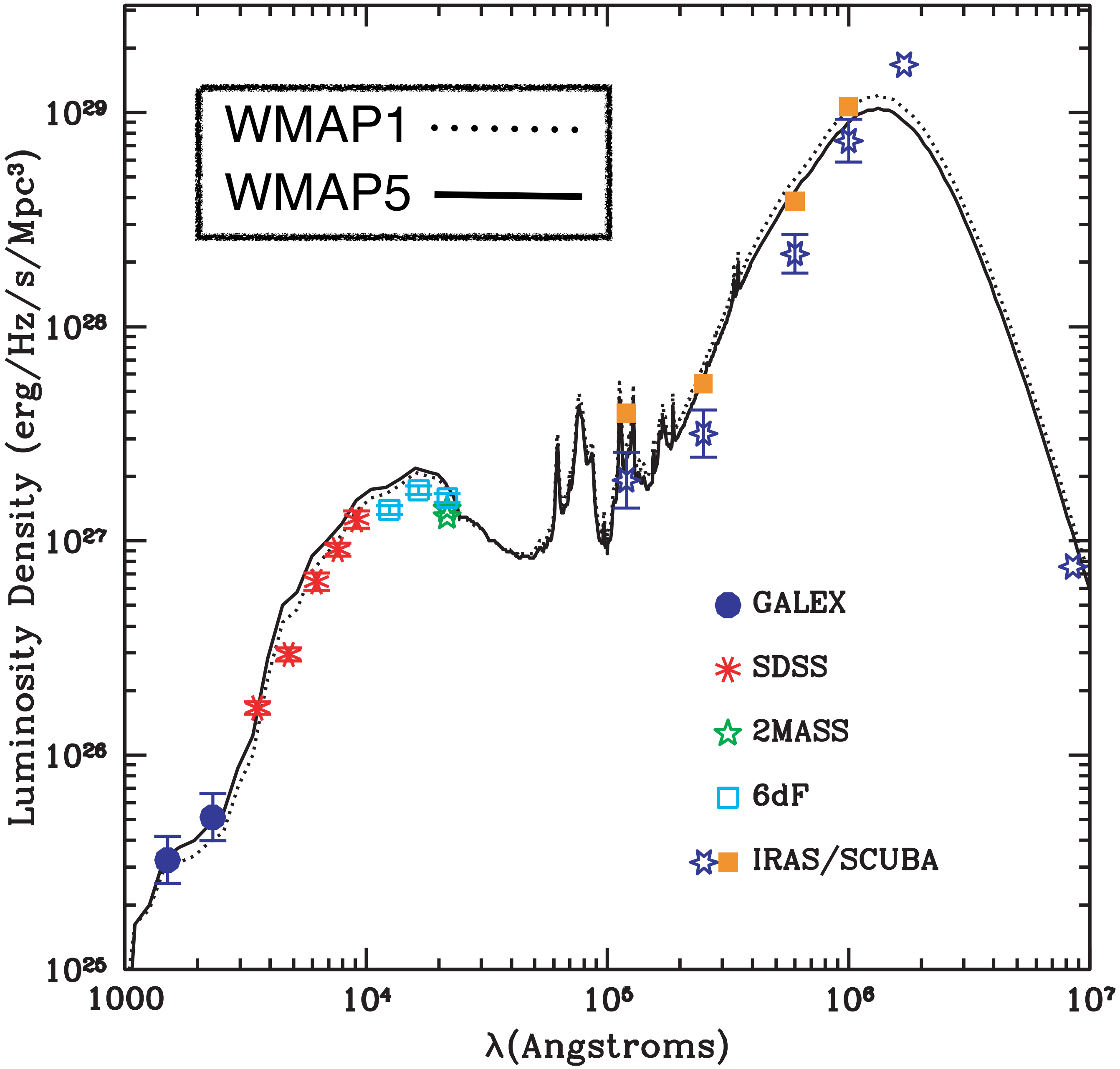

Evolving Luminosity Density

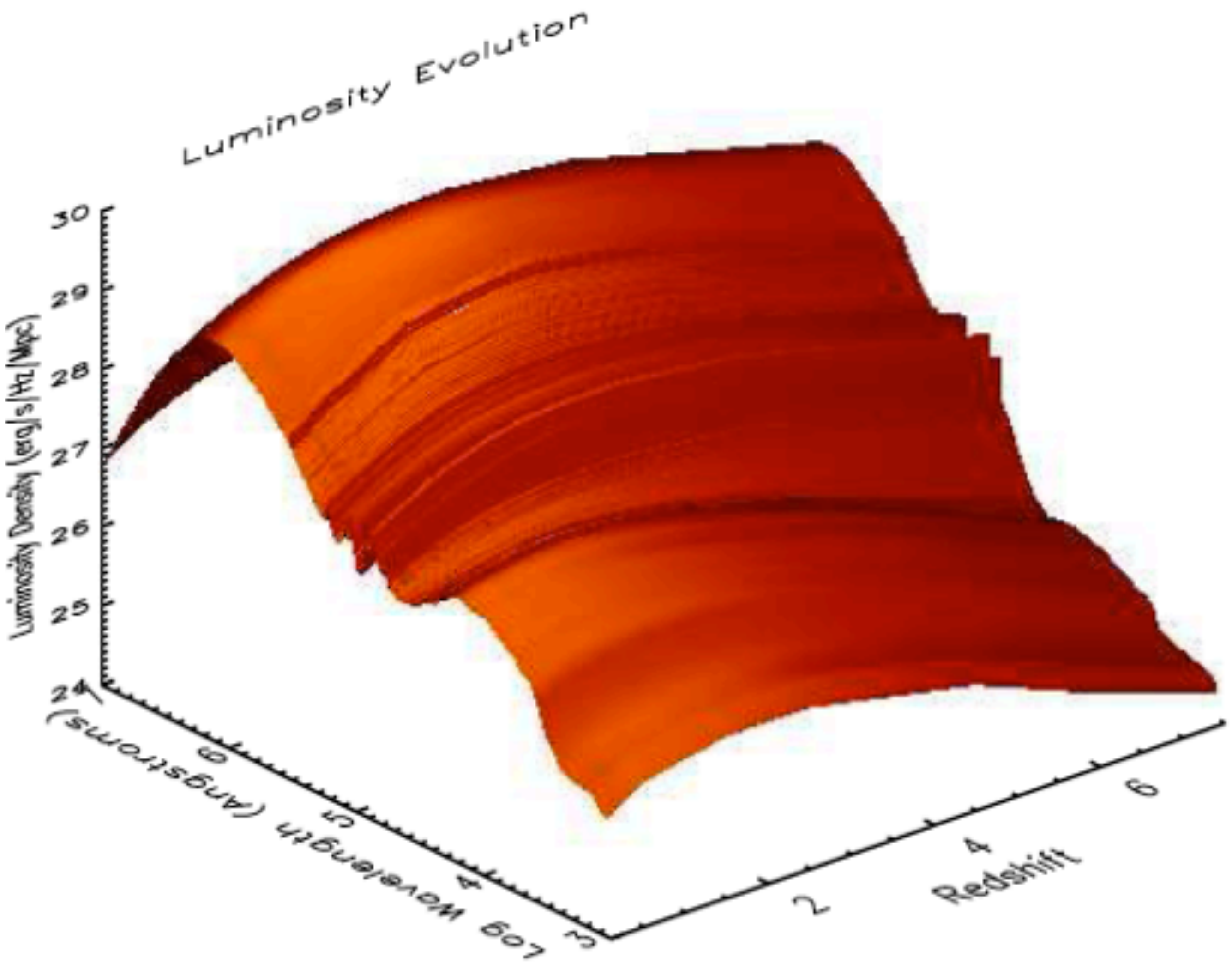

Gilmore, Somerville, Primack, & Domínguez (2012)

Some Results from our Semi-Analytic Models

Evolving Luminosity Functions

B-band

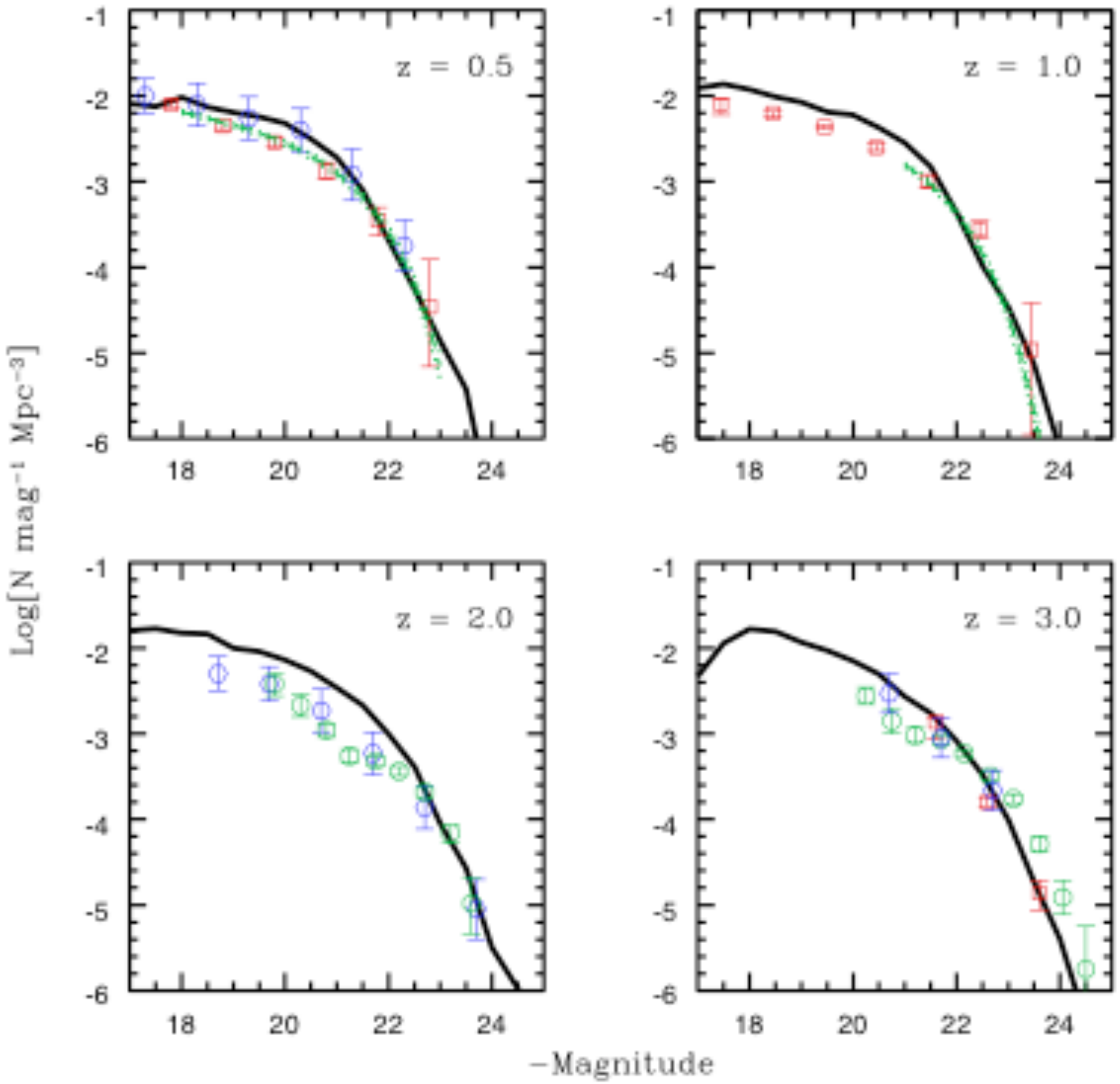

K-band

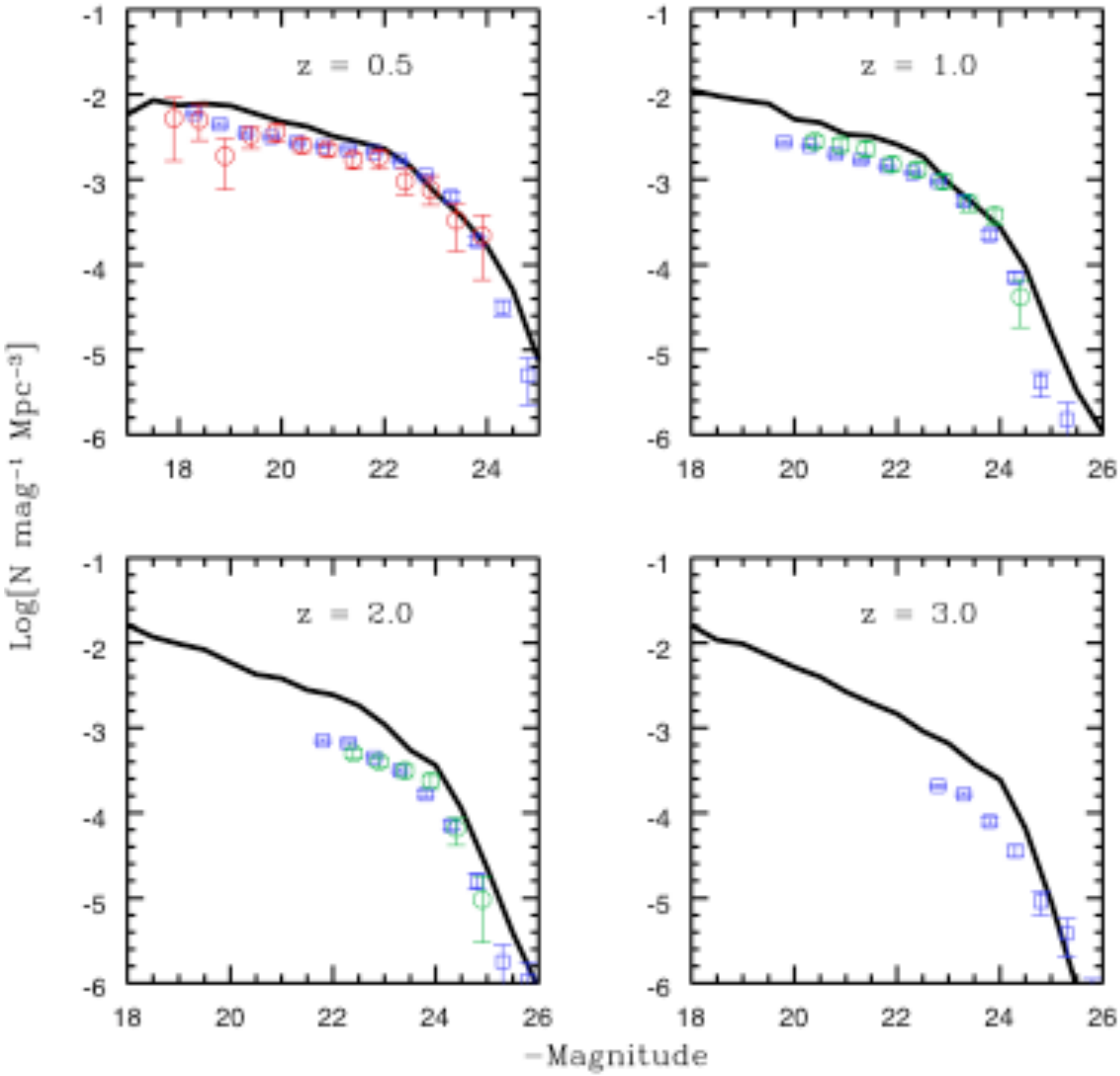

An advantage of the SAM approach is that it is possible to compare predictions and observations at all redshifts and in all spectral bands.

Gilmore, Somerville, Primack, & Domínguez (2012)

Some Results from our Semi-Analytic Models

Number Counts in UV, b, v, i, and z Bands

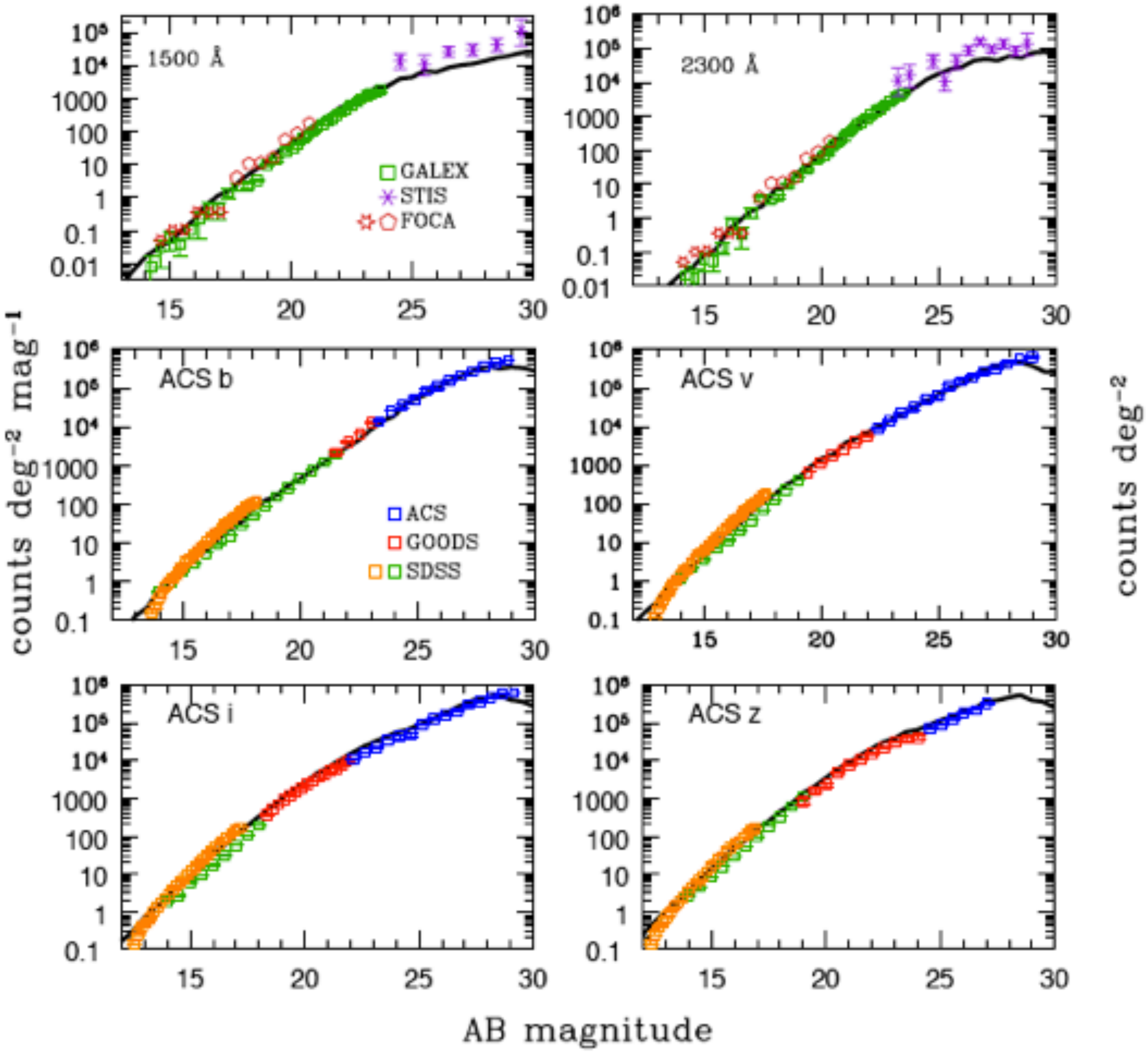

3.6, 8, 24 and 24, 70, 160, & 850 µm Bands

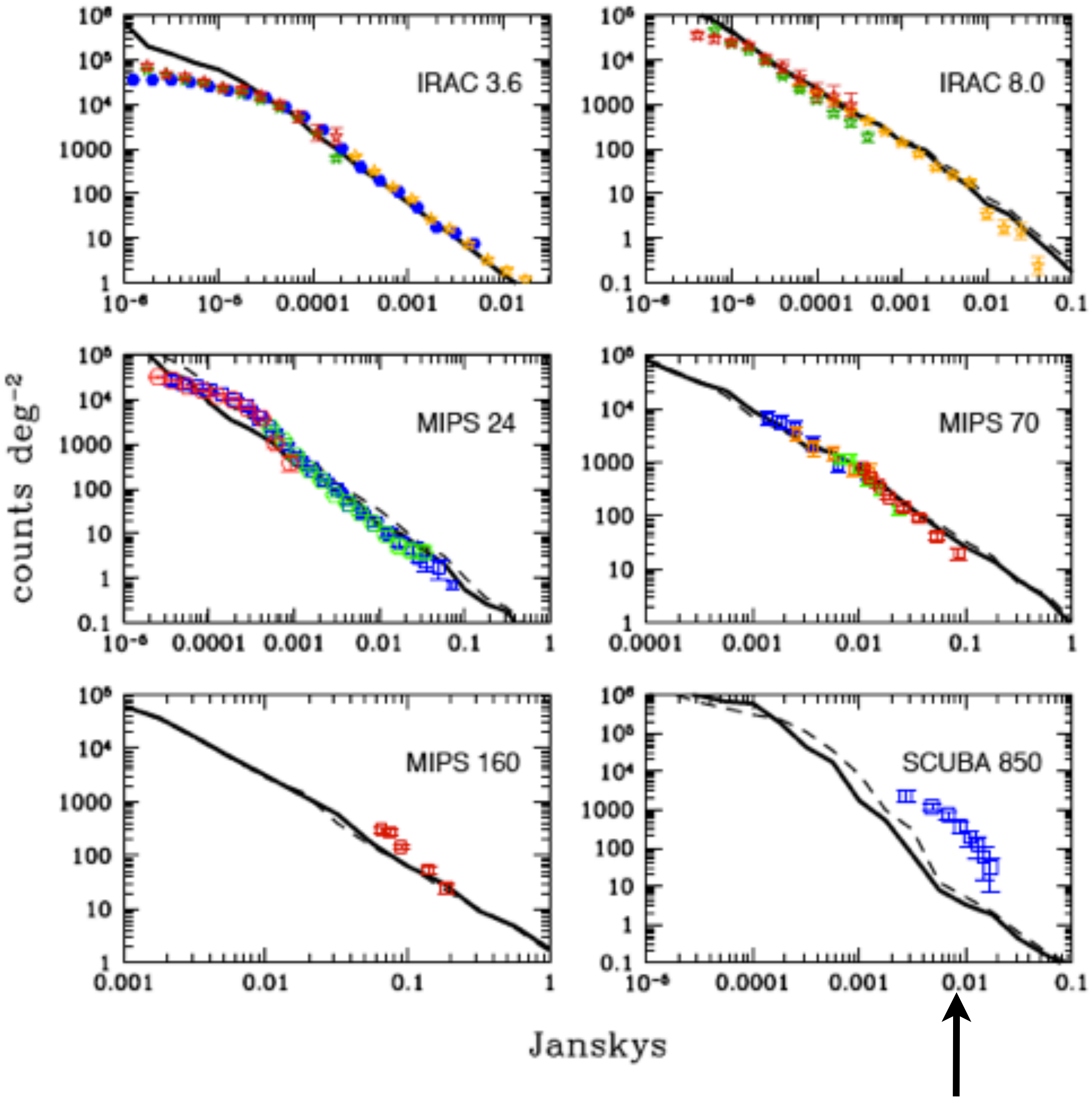

Somerville, Gilmore, Primack, & Domínguez (2012)

Worst failure is at 850 μm

EBL from our Semi-Analytic Models

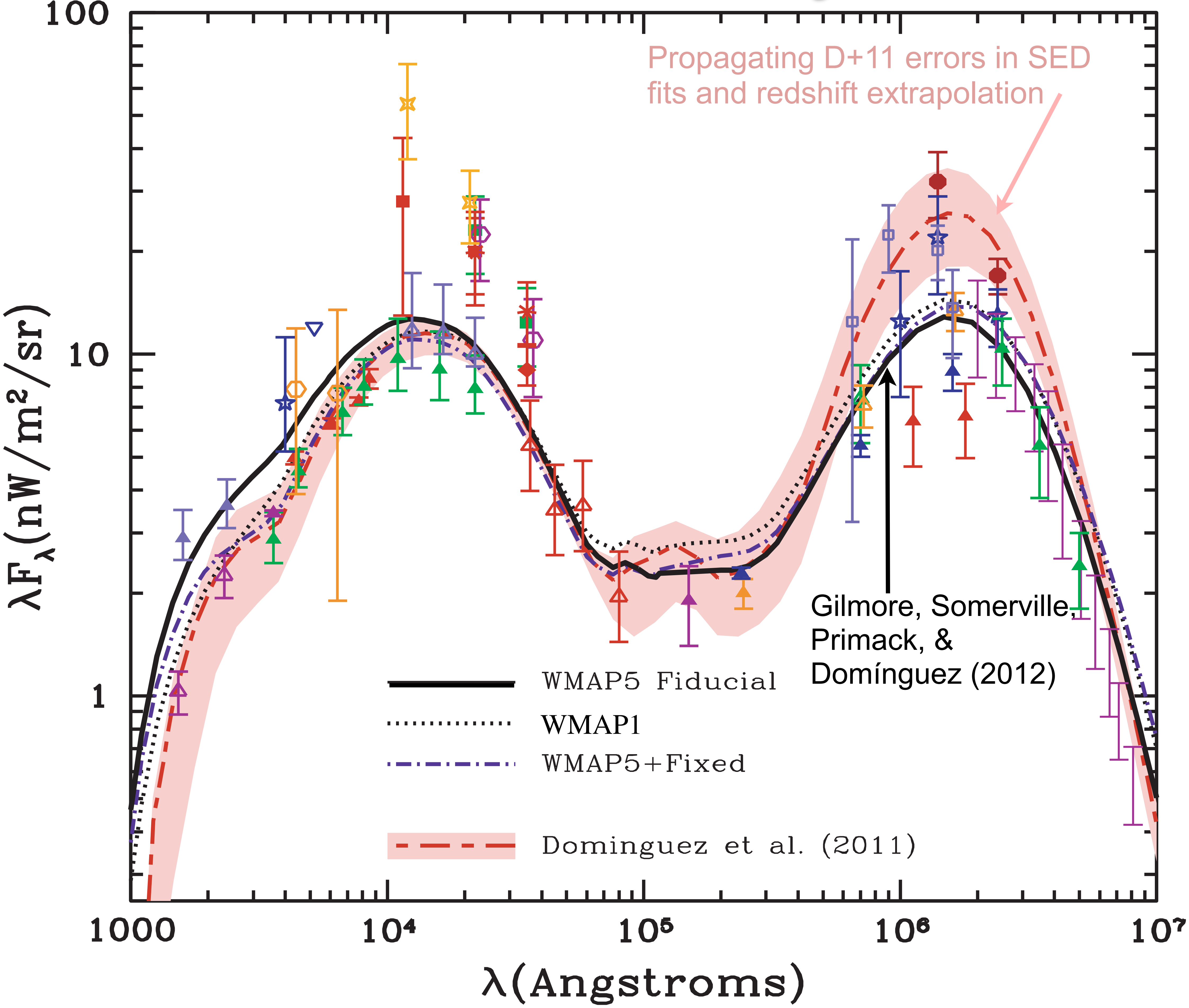

Propagating D+11 errors in SED fits and redshift extrapolation

Gilmore, Somerville, Primack, & Domínguez (2012)

Evolution of the EBL

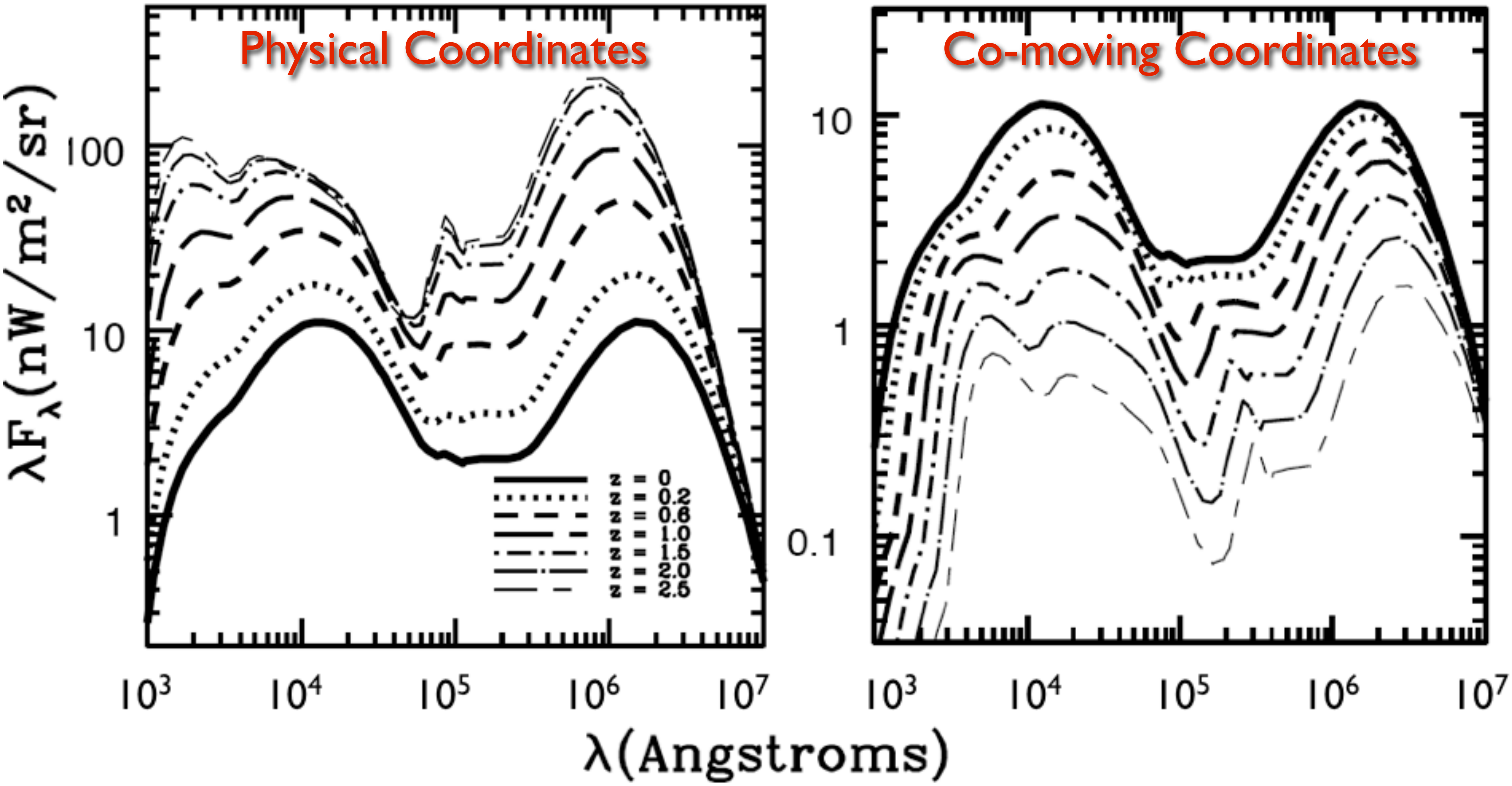

The evolution of the EBL in our WMAP5 Fiducial model. This is plotted on the left panel in standard units. The right panel shows the build-up of the present-day EBL by plotting the same quantities in comoving units. The redshifts from 0 to 2.5 are shown by the different line types in the key in the left panel.

Gilmore, Somerville, Primack, & Domínguez (2012)

Predicted Gamma Ray Attenuation

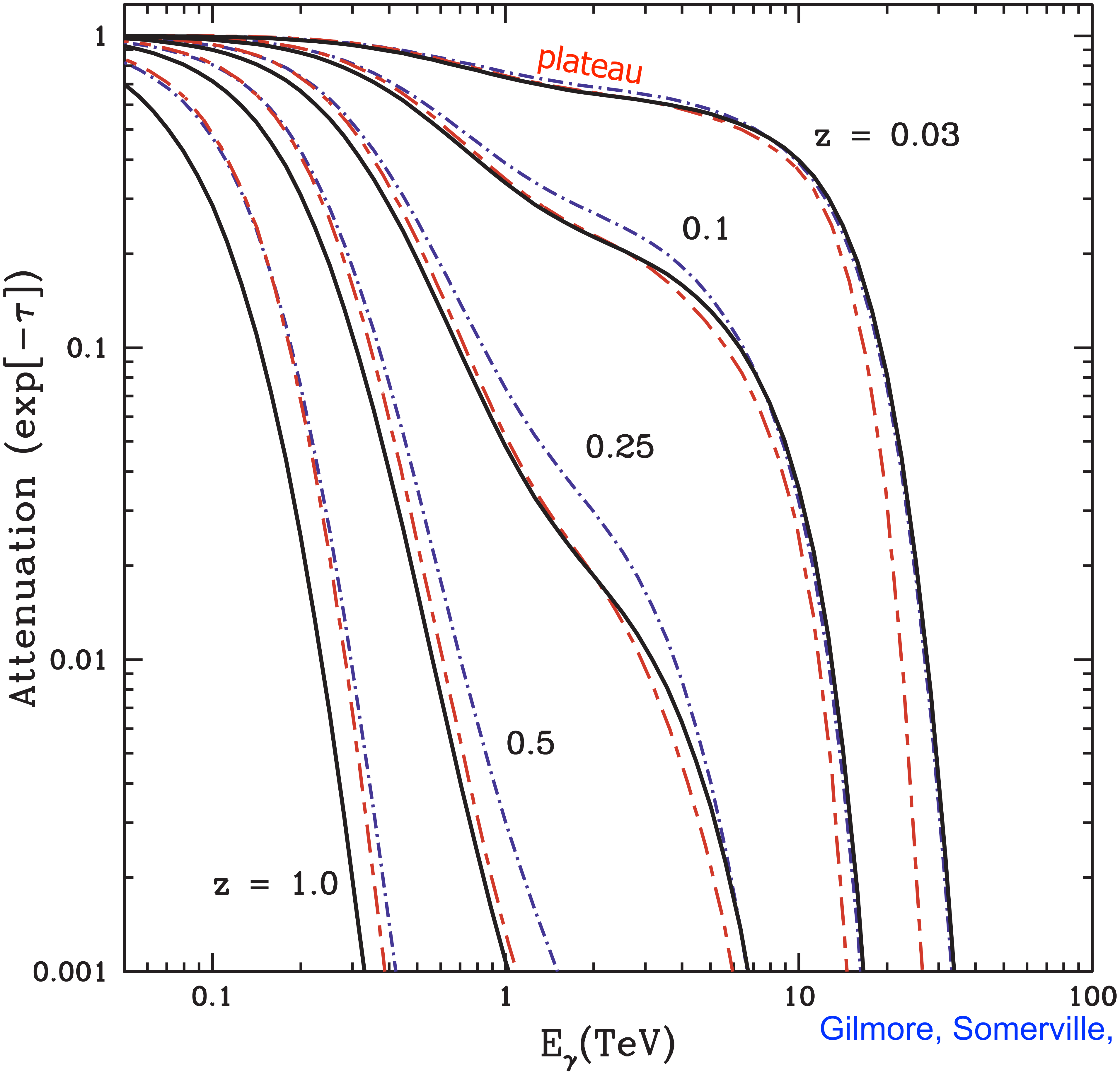

Increasing distance causes absorption features to increase in magnitude and appear at lower energies. The plateau seen between 1 and 10 TeV at low z is a product of the mid-IR valley in the EBL spectrum.

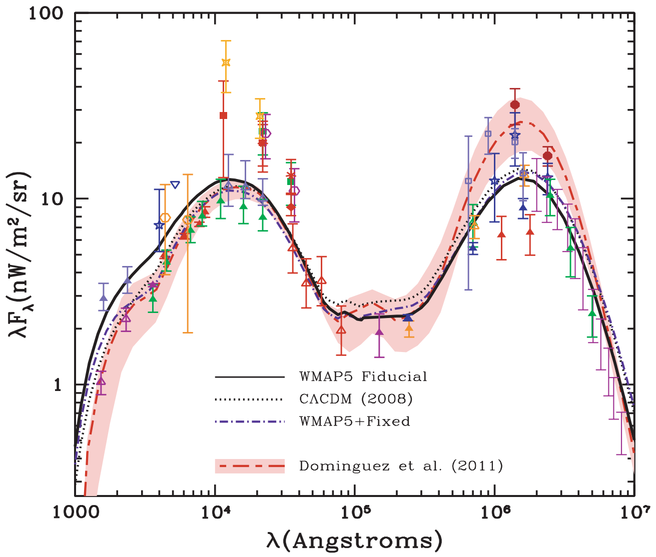

Gilmore, Somerville, Primack, & Domínguez (2012)

Gamma Ray Attenuation due to γγ → e+e-

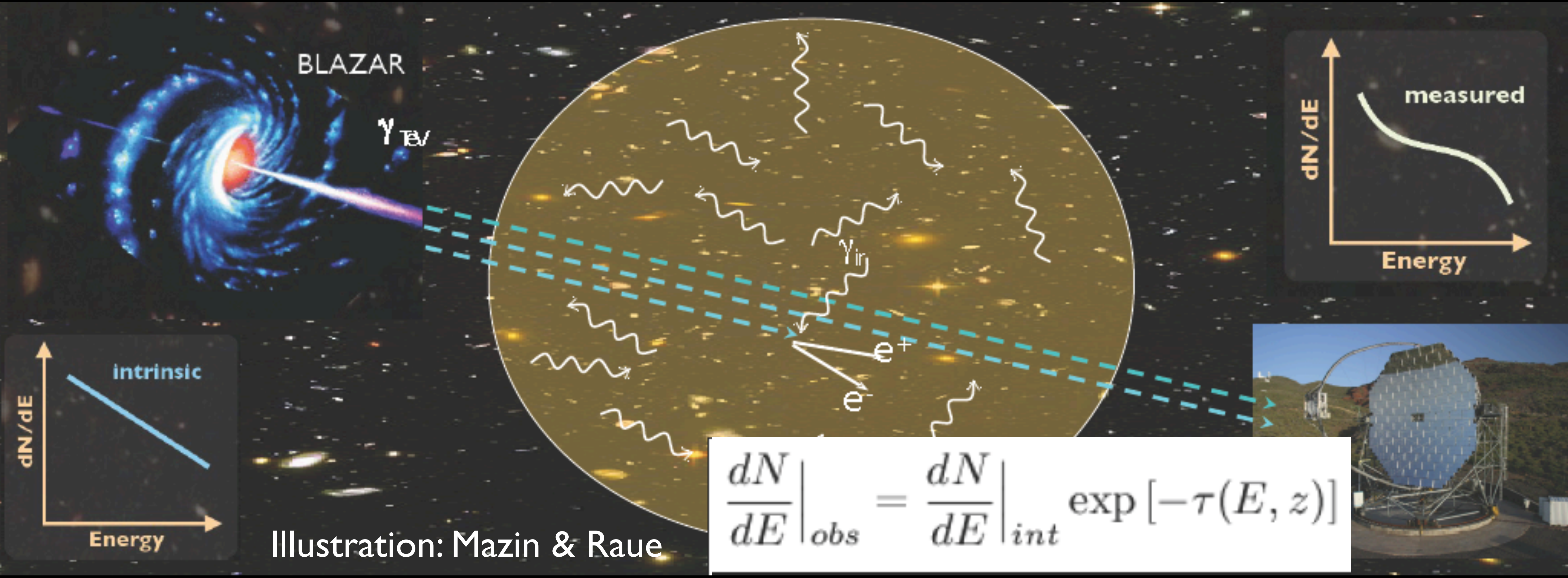

Illustration: Mazin & Raue

$$\left.\frac{dN}{dE}\right|_{obs} = \left.\frac{dN}{dE}\right|_{int} \exp\left[-\tau(E,z)\right]$$

If we know the intrinsic spectrum, we can infer the optical depth $\tau(E,z)$ from the observed spectrum. In practice, we typically *assume* that $dN/dE|_{int}$ is not harder than $E^{-\Gamma}$ with $\Gamma = 1.5$, since local sources have $\Gamma \geq 2$. More conservatively, we can assume that $\Gamma \geq 2/3$.

Reconstructed Blazar Spectral Indexes

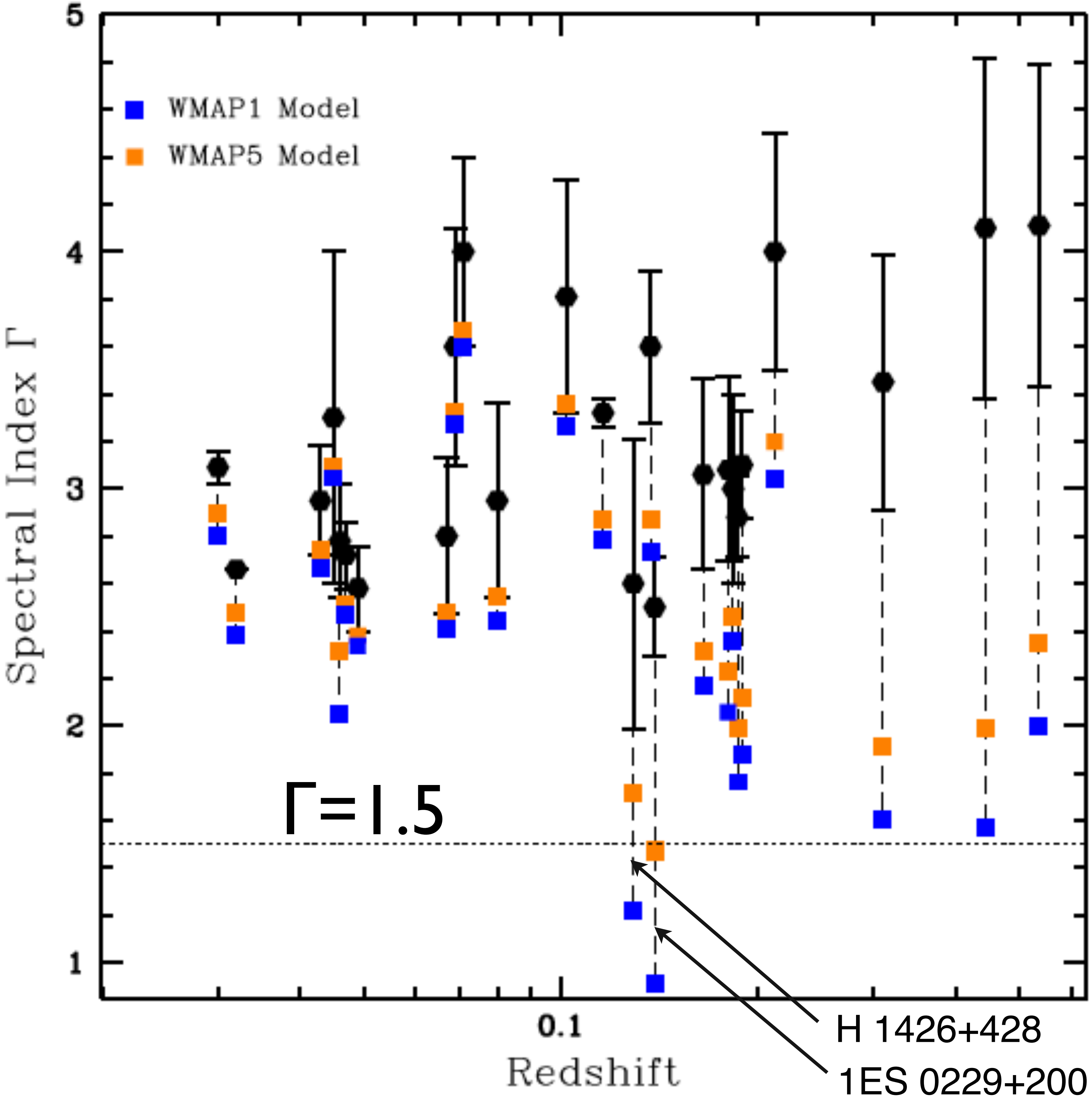

With our SAM based on WMAP5 cosmological parameters and Spitzer (Rieke+09) dust emission templates, all high redshift blazars have intrinsic spectral indexes Γ≥1.5, as expected from nearby sources.

(Of course, the spectrum could be harder than Γ≥1.5.)

Predicted Gamma Ray Attenuation

The Cosmic Gamma Ray Horizon is the observed gamma ray energy as a function of redshift where the attenuation is 1/e = 0.368

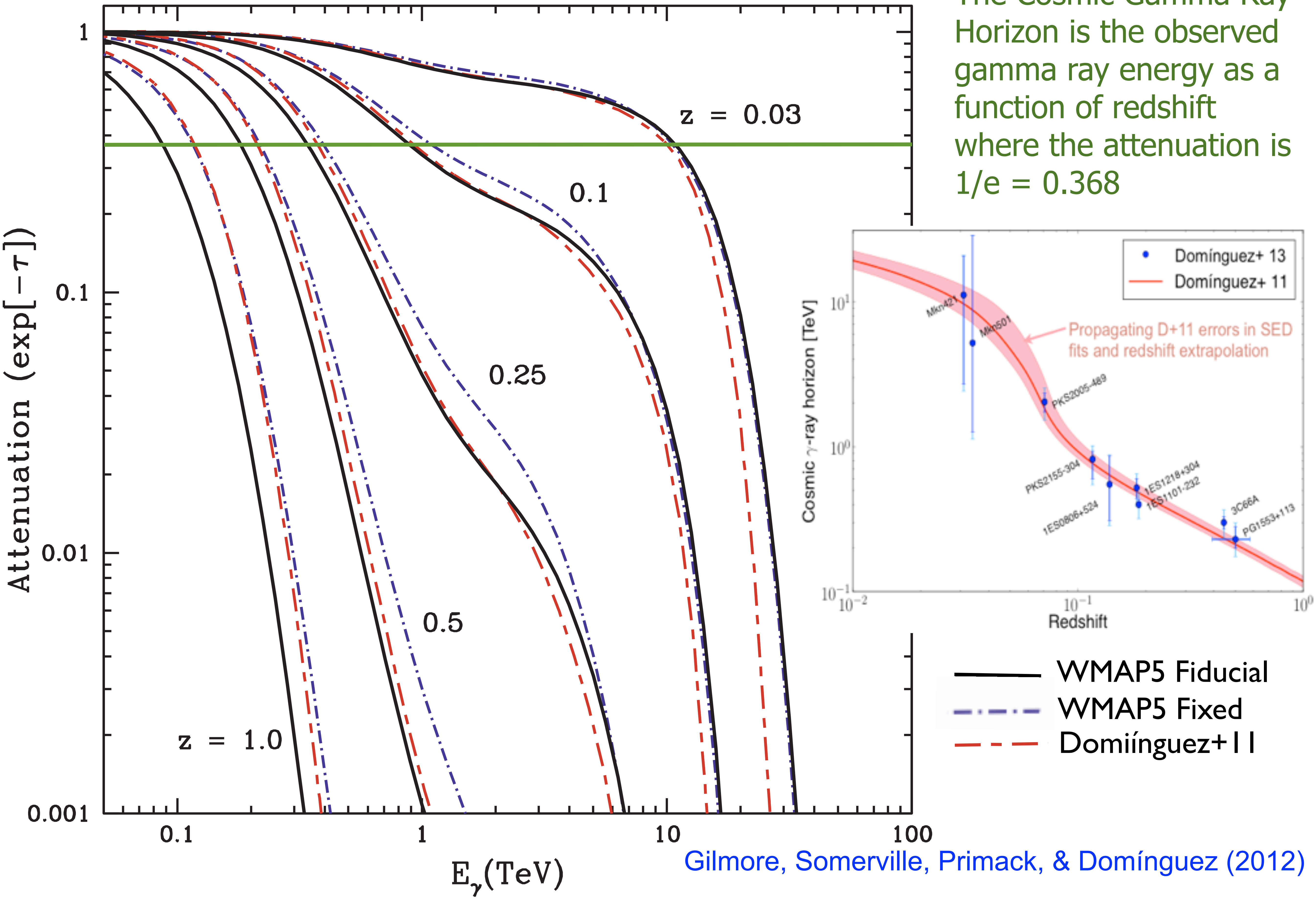

Gilmore, Somerville, Primack, & Domínguez (2012)

Cosmic Gamma-Ray Horizon

With a 50 GeV threshold, we see to z≈1.5-3 with less than 1/e attenuation!

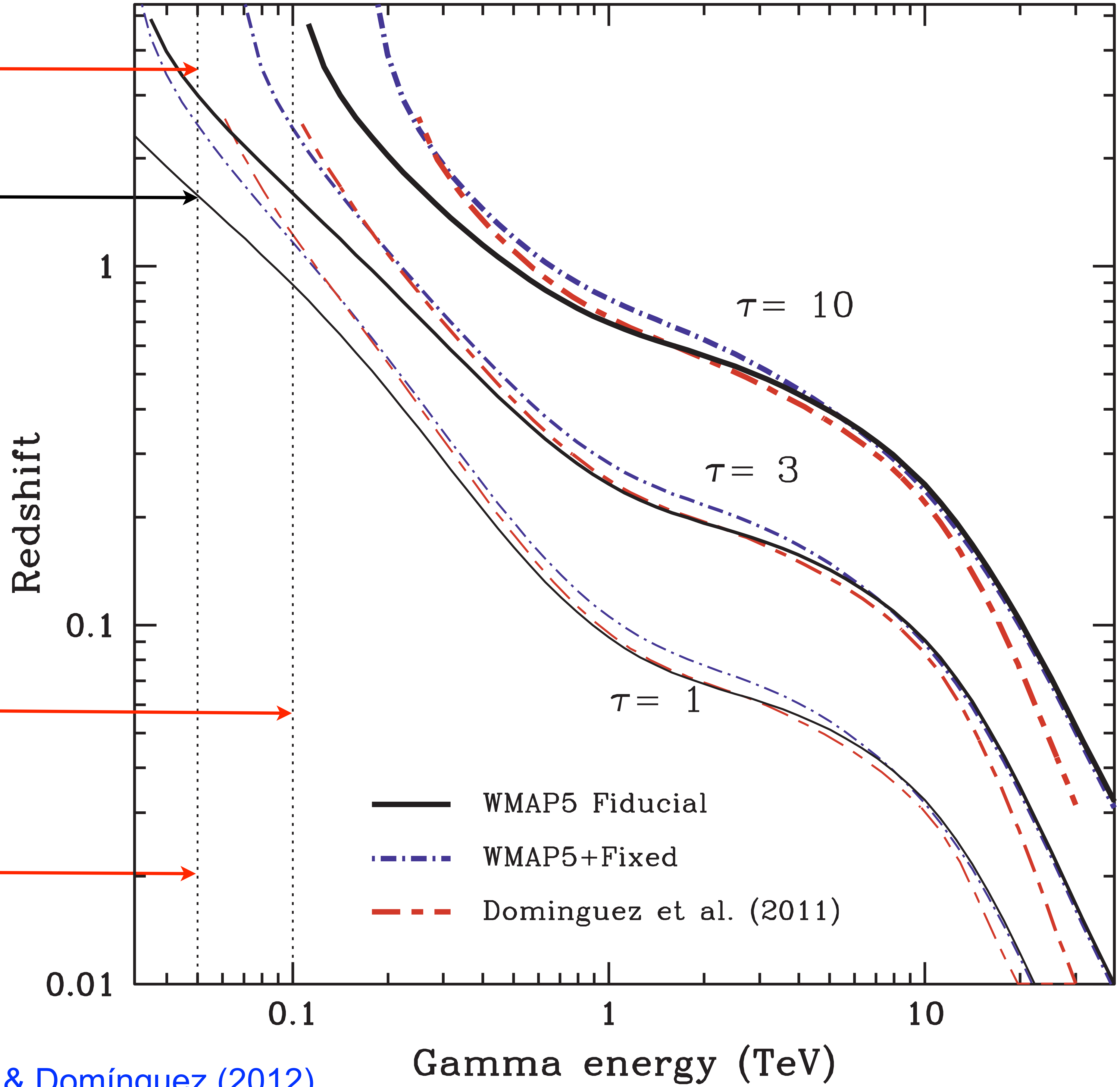

100 GeV Threshold

50 GeV Threshold

Gilmore, Somerville, Primack, & Domínguez (2012)

DETECTION OF THE COSMIC γ-RAY HORIZON FROM MULTIWAVELENGTH OBSERVATIONS OF BLAZARS

ApJ 770, 77 (2013)

A. Domínguez, J. D. Finke, F. Prada, J. R. Primack, F. S. Kitaura, B. Siana, D. Paneque

The first statistically significant detection of the cosmic γ-ray horizon (CGRH) that is independent of any extragalactic background light (EBL) model is presented. The CGRH is a fundamental quantity in cosmology. It gives an estimate of the opacity of the Universe to very-high energy (VHE) γ-ray photons due to photon-photon pair production with the EBL. The only estimations of the CGRH to date are predictions from EBL models and lower limits from γ-ray observations of cosmological blazars and γ-ray bursts. Here, we present synchrotron self-Compton models (SSC) of the spectral energy distributions of 15 blazars based on (almost) simultaneous observations from radio up to the highest energy γ-rays taken with the Fermi satellite. These SSC models predict the unattenuated VHE fluxes, which are compared with the observations by imaging atmospheric Cherenkov telescopes. This comparison provides an estimate of the optical depth of the EBL, which allows a derivation of the CGRH through a maximum likelihood analysis that is EBL-model independent. We find that the observed CGRH is compatible with the current knowledge of the EBL.

SED multiwavelength fits

A one-zone synchrotron/SSC model is fit to the multiwavelength data excluding the Cherenkov data, which are EBL attenuated. Then, this fit is extrapolated to the VHE regime representing the intrinsic VHE spectrum. Technique similar to Mankuzhiyil et al. 2010.

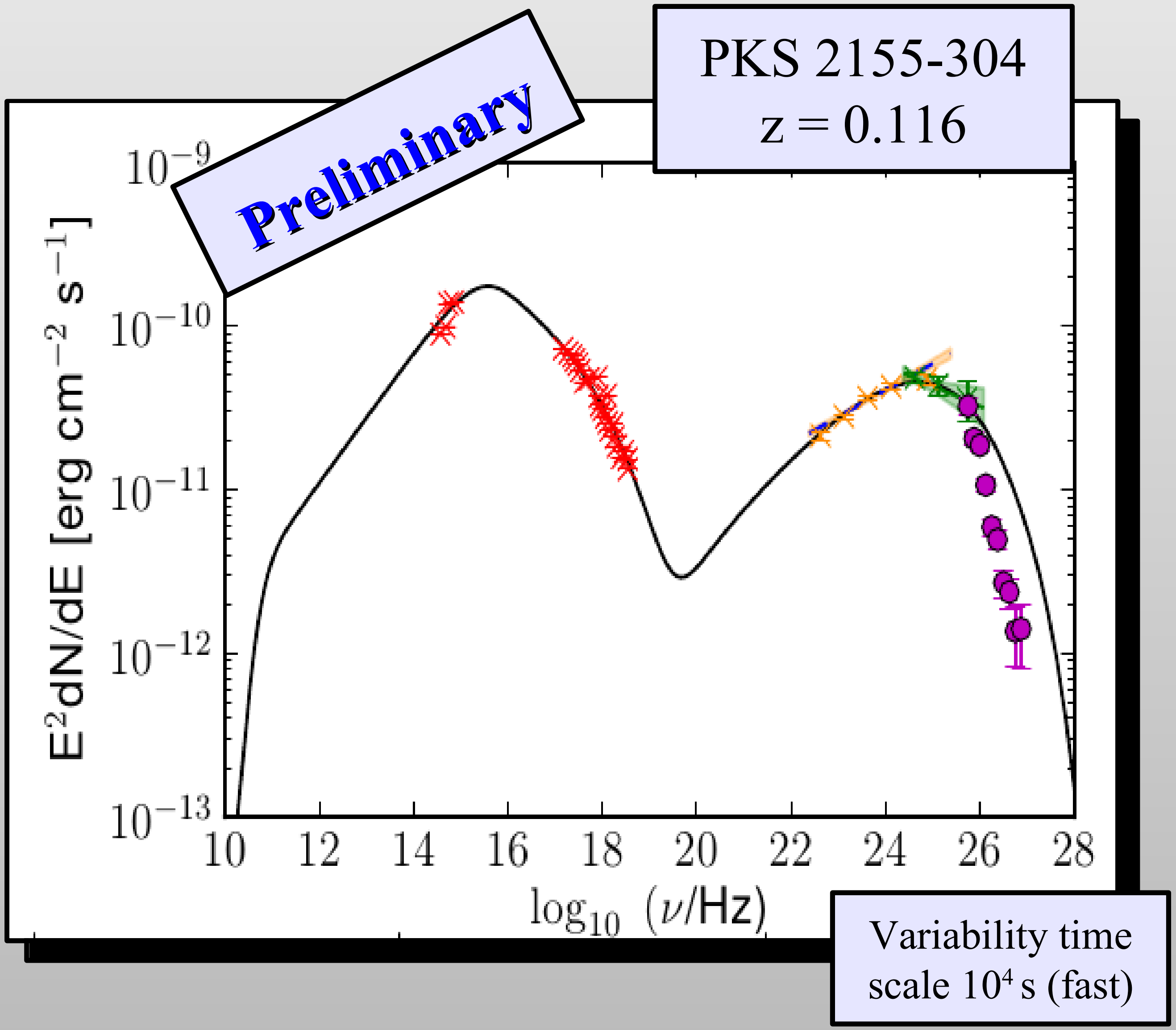

PKS 2155-304
z = 0.116

Variability time scale 10^4 s (fast)

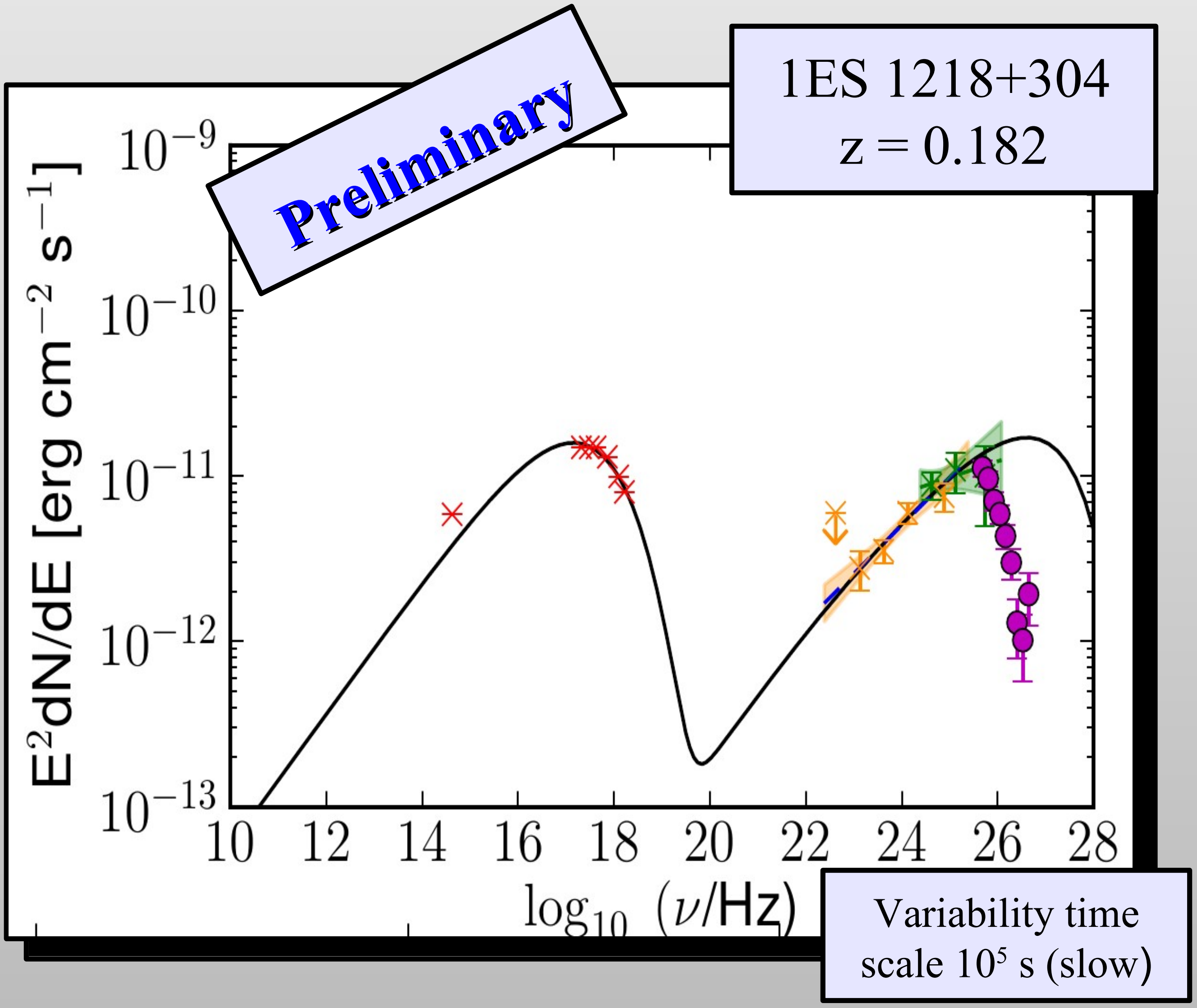

1ES 1218+304
z = 0.182

Variability time scale 10^5 s (slow)

Domínguez+13

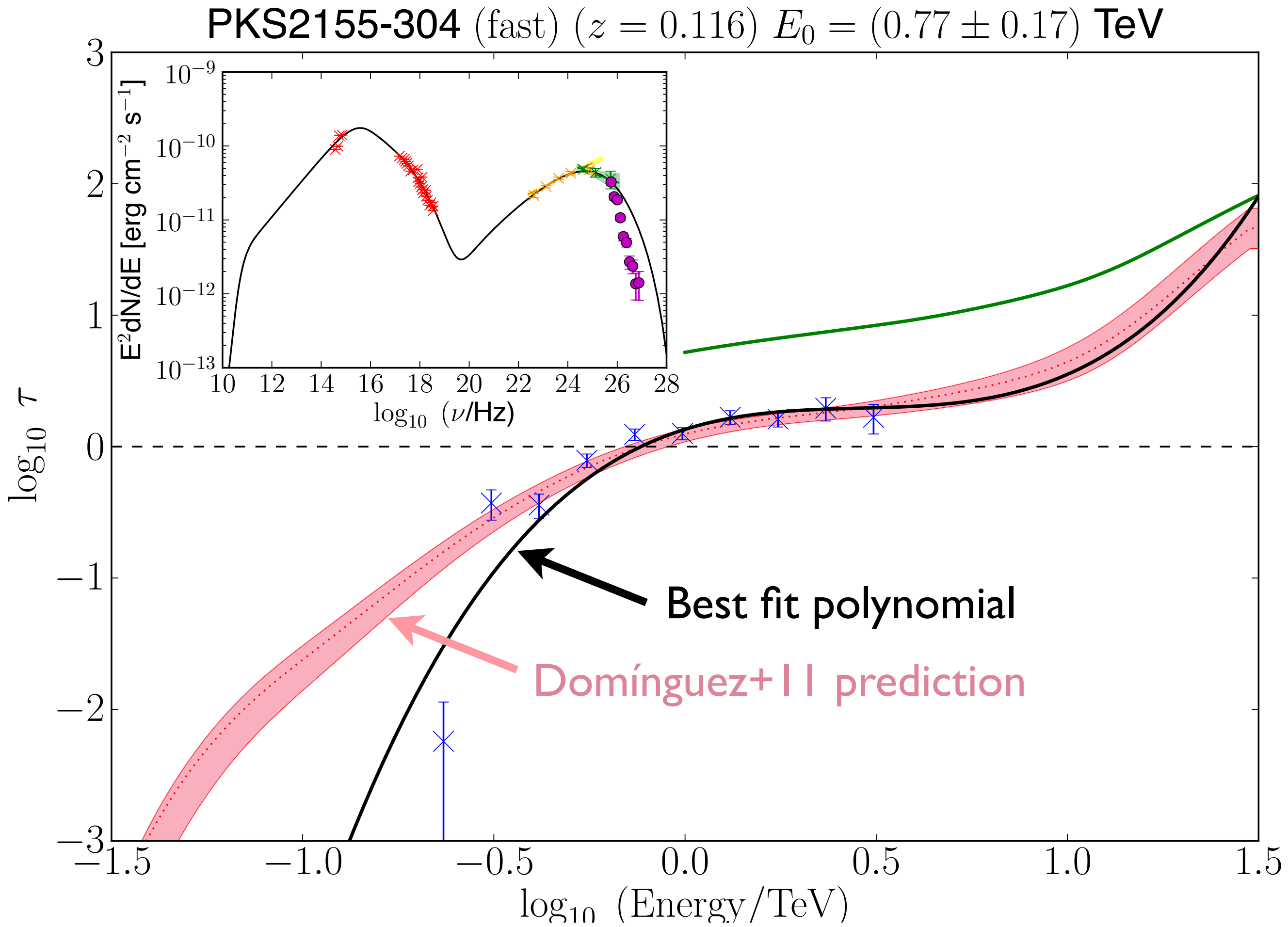
PKS2155-304 (fast) ($z = 0.116$) $E_0 = (0.77 \pm 0.17)$ TeV

Best fit polynomial

Domínguez+11 prediction

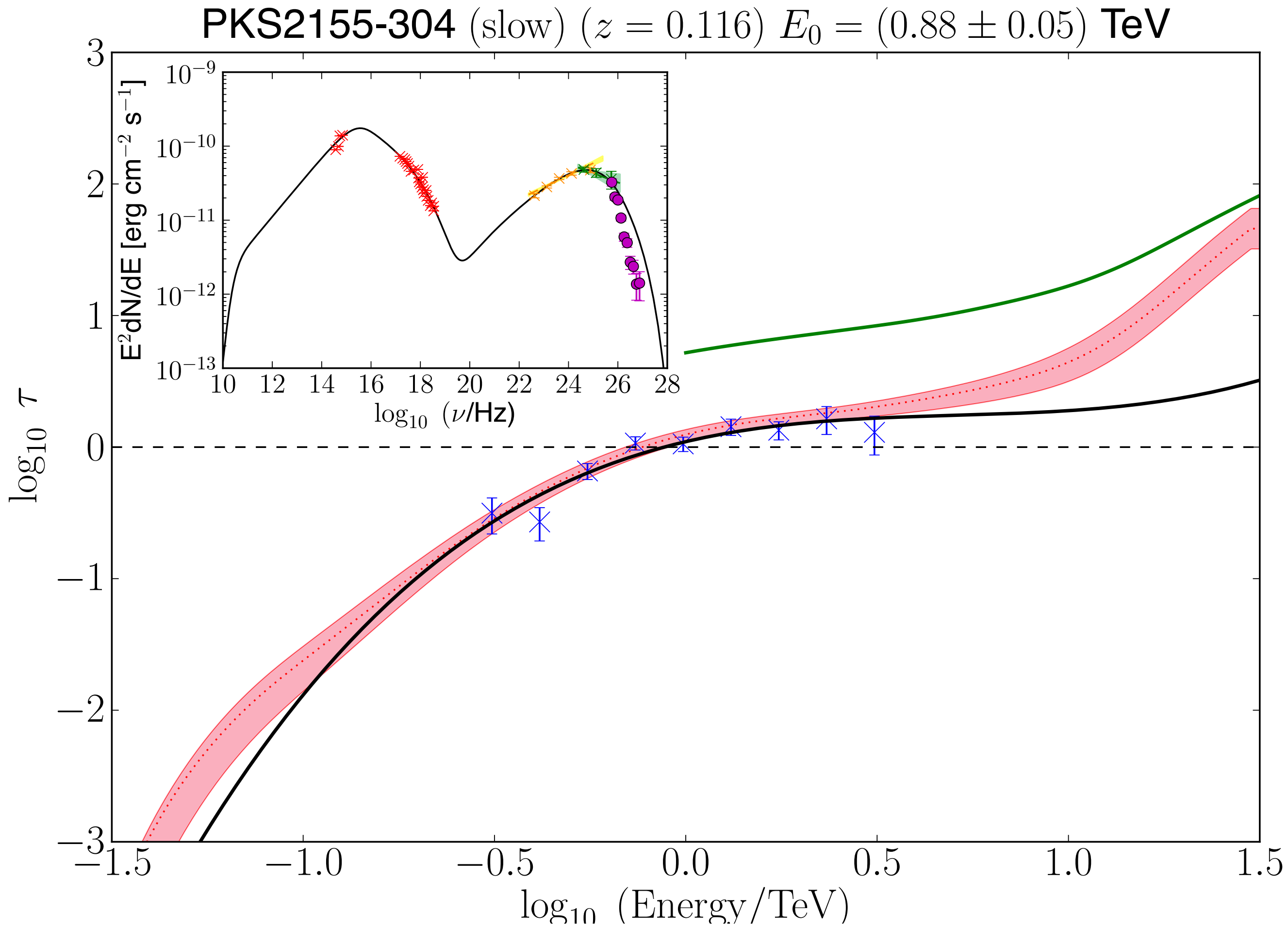
PKS2155-304 (slow) ($z = 0.116$) $E_0 = (0.88 \pm 0.05)$ TeV

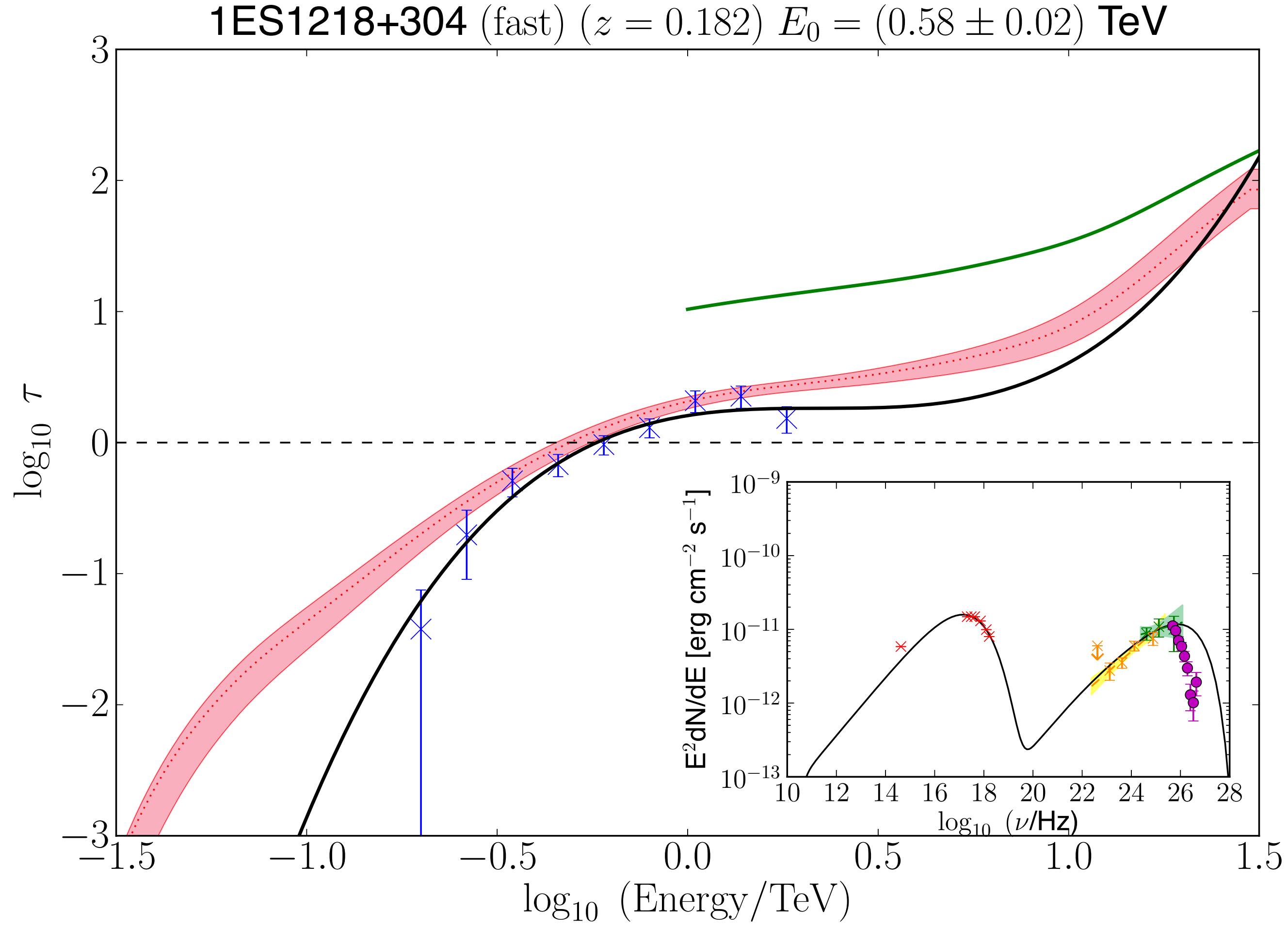
1ES1218+304 (fast) ($z = 0.182$) $E_0 = (0.58 \pm 0.02)$ TeV

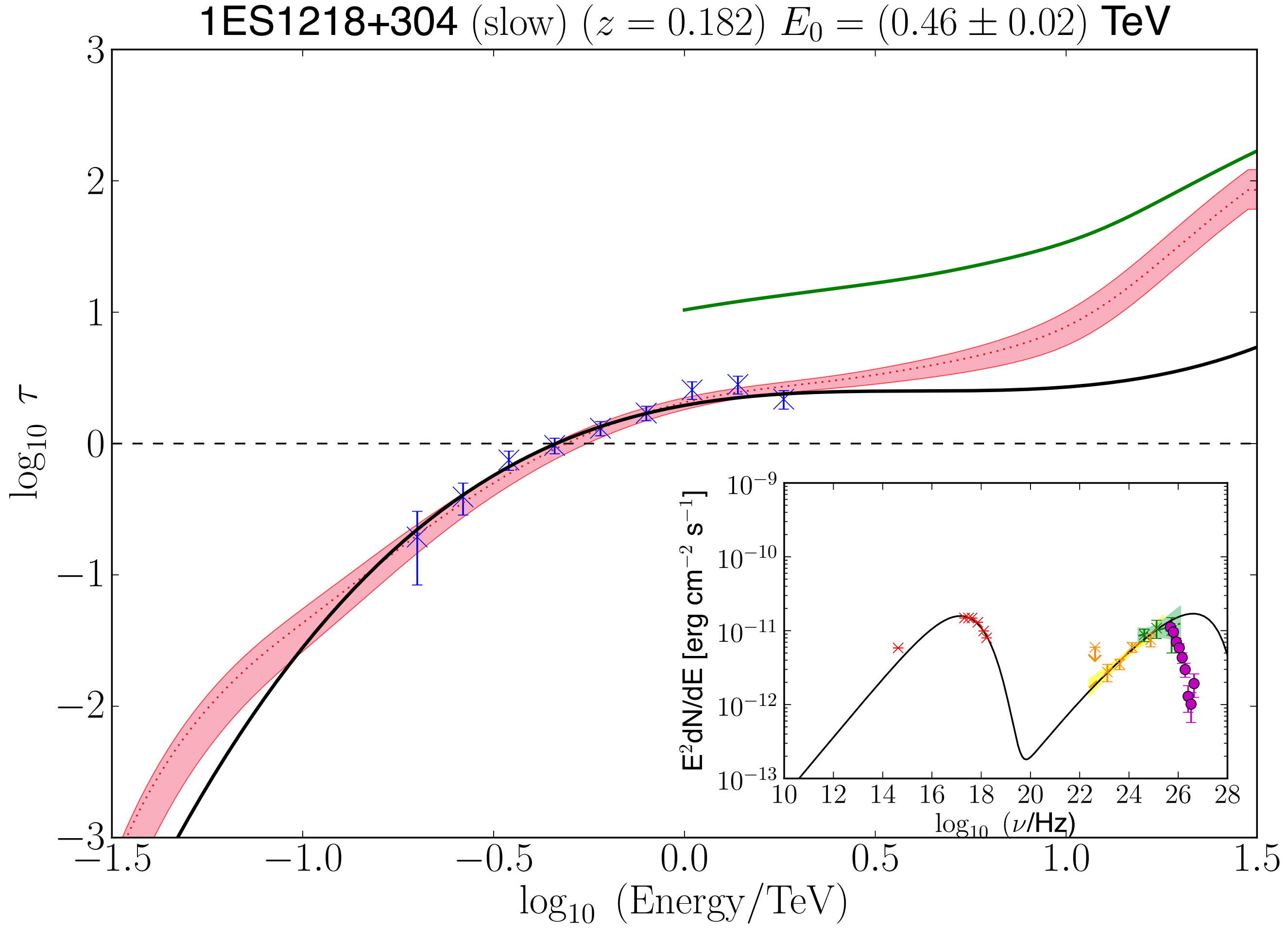
1ES1218+304 (slow) ($z = 0.182$) $E_0 = (0.46 \pm 0.02)$ TeV

Quasi-Simultaneous Catalog of 15 BL Lacs

(based on the compilation by Zhang et al. 2012)

Source	Redshift	$E_0 \pm (\Delta E_0)_{stat} \pm (\Delta E_0)_{sys}$ [TeV]	$E_{D11} \pm \Delta E_{D11}$ [TeV]
Mkn 421	0.031	$11.14^{+9.56}_{-8.44} \pm 2.23$	$9.72^{+1.85}_{-3.17}$
Mkn 501	0.034	$5.20^{+23.49}_{-3.94} \pm 1.04$	$8.75^{+1.68}_{-3.31}$
1ES 2344+514	0.044	None	$6.01^{+1.20}_{-3.23}$
1ES 1959+650	0.048	None	$5.12^{+1.02}_{-2.99}$
PKS 2005−489	0.071	$2.04^{+0.30}_{-0.31} \pm 0.41$	$1.83^{+0.34}_{-1.06}$
W Comae	0.102	None	$0.90^{+0.09}_{-0.18}$
PKS 2155−304	0.116	$0.82^{+0.11}_{-0.22} \pm 0.16$	$0.77^{+0.07}_{-0.13}$
H 1426+428	0.129	None	$0.68^{+0.06}_{-0.11}$
1ES 0806+524	0.138	$0.55^{+0.31}_{-0.24} \pm 0.11$	$0.64^{+0.05}_{-0.10}$
H 2356-309	0.165	None	$0.54^{+0.04}_{-0.07}$
1ES 1218+304	0.182	$0.52^{+0.08}_{-0.08} \pm 0.10$	$0.49^{+0.04}_{-0.06}$
1ES 1101−232	0.186	$0.40^{+0.03}_{-0.02} \pm 0.08$	$0.48^{+0.04}_{-0.06}$
1ES 1011+496	0.212	None	$0.43^{+0.03}_{-0.05}$
3C 66A	0.444	$0.30^{+0.03}_{-0.03} \pm 0.06$	$0.23^{+0.02}_{-0.02}$
PG 1553+113	$0.500^{+0.080}_{-0.105}$	$0.23^{+0.05}_{-0.03} \pm 0.05$	$0.21^{+0.02}_{-0.02}$

E_0 is the CGRH (i.e., the energy at which the optical depth $\tau = 1$) and E_{D11} is the energy where $\tau = 1$ for the Fiducial model of Domínguez, Primack, et al. 2011. None means that our methodology output no solution for the CGHR, usually because the SSC model failed.

Domínguez+13

DETECTION OF THE COSMIC γ-RAY HORIZON FROM MULTIWAVELENGTH OBSERVATIONS OF BLAZARS

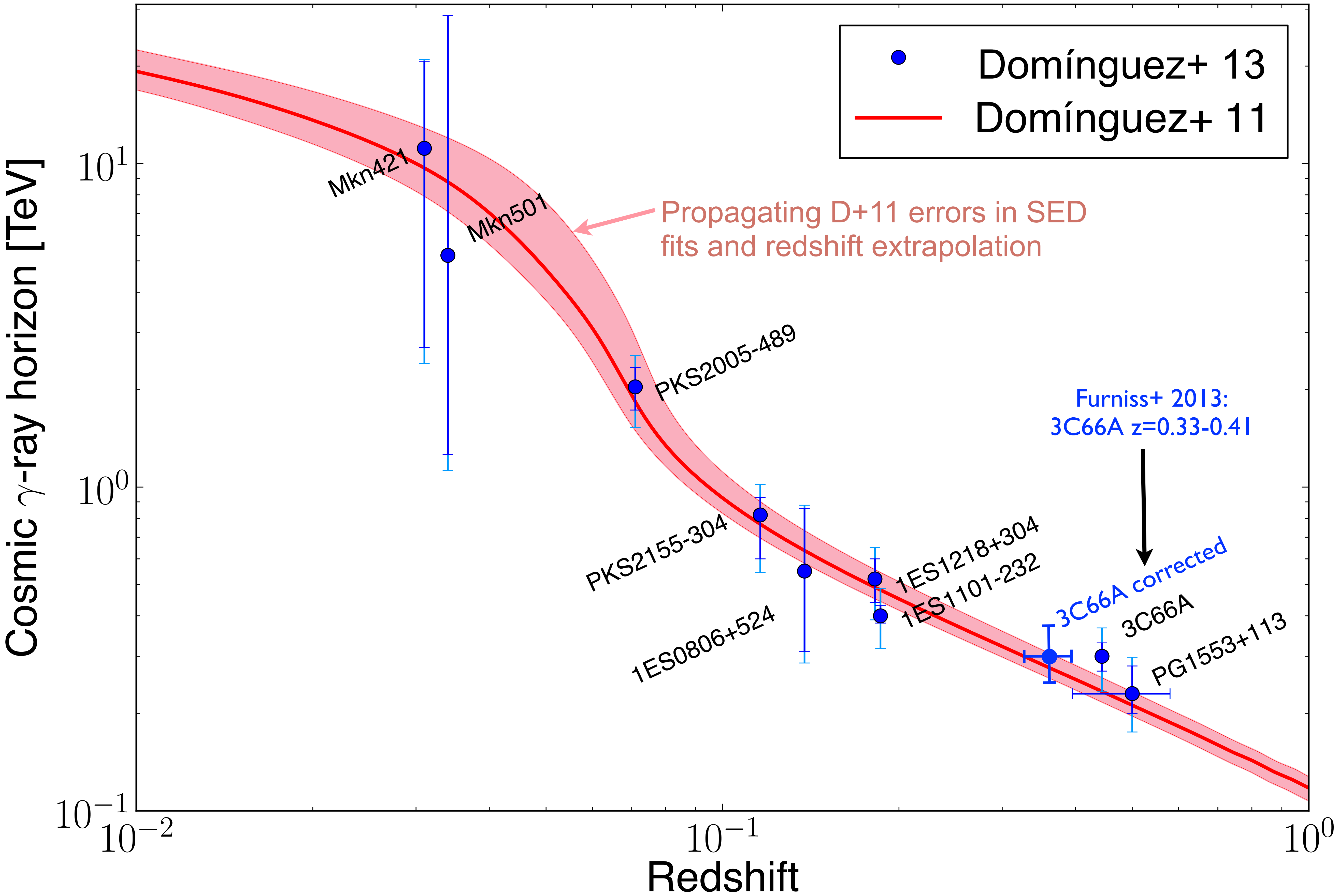

Propagating D+11 errors in SED fits and redshift extrapolation

Furniss+ 2013:
3C66A z=0.33-0.41

The Imprint of the Extragalactic Background Light in the Gamma-Ray Spectra of Blazars

M. Ackermann, M. Ajello, et al. (Fermi), *Science* 338, 1190 (2012)

ABSTRACT The light emitted by stars and accreting compact objects through the history of the universe is encoded in the intensity of the extragalactic background light (EBL). Knowledge of the EBL is important to understand the nature of star formation and galaxy evolution, but direct measurements of the EBL are limited by galactic and other foreground emissions. Here, we report an absorption feature seen in the combined spectra of a sample of gamma-ray blazars out to a redshift of $z \sim 1.6$. This feature is caused by attenuation of gamma rays by the EBL at optical to ultraviolet frequencies and allowed us to measure the EBL flux density in this frequency band.

Fig. 1. Measurement, at the 68 and 95% confidence levels (including systematic uncertainties added in quadrature), of the opacity $\tau_{\gamma\gamma}$ from the best fits to the Fermi data compared with predic- tions of EBL models. The plot shows the measurement at $z \approx 1$, which is the average redshift of the most constraining redshift interval (i.e., $0.5 \lesssim z < 1.6$). The Fermi-LAT measurement was derived com- bining the limits on the best-fit EBL models. The downward arrow represents the 95% upper limit on the opacity at $z = 1.05$ derived in A. A. Abdo et al., Astrophys. J. 723, 1082 (2010).

.

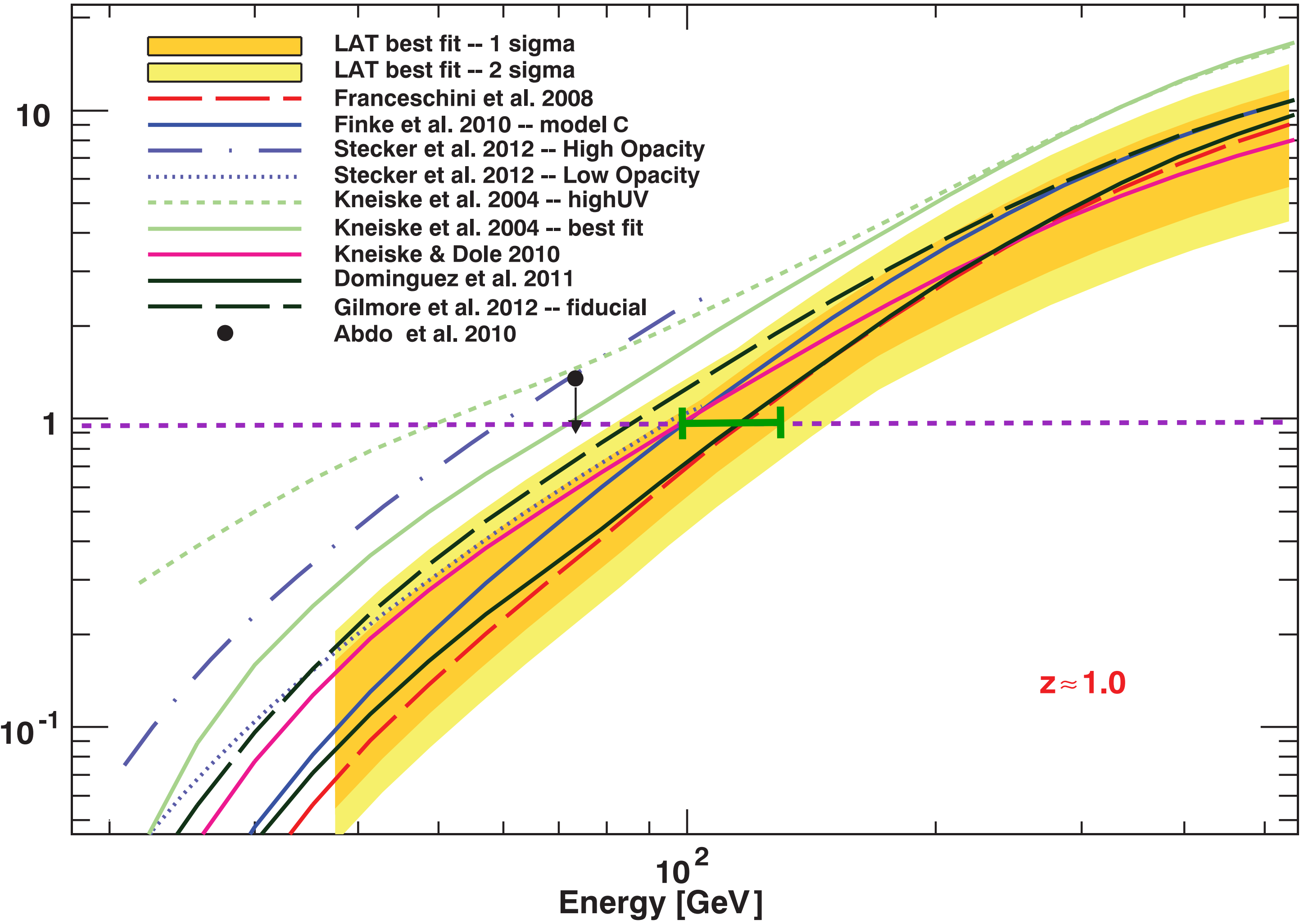

M. Ackermann, M. Ajello, et al. (Fermi), Science 338, 1190 (2012)

Measurement of Tau with Energy and Redshift

- We use the composite likelihood in small energy bins to measure the collective deviation of the observed spectra from the intrinsic ones

- The cut-off moves in z and energy as expected for EBL absorption (for low opacity models)

- It is difficult to explain this attenuation with an intrinsic property of BL Lacs
  1. BL Lacs required to evolve across the z=0.2 barrier
  2. Attenuation change with energy and redshift cannot be explained by an intrinsic cut-off that changes from source to source because of redshift and blazar sequence effects

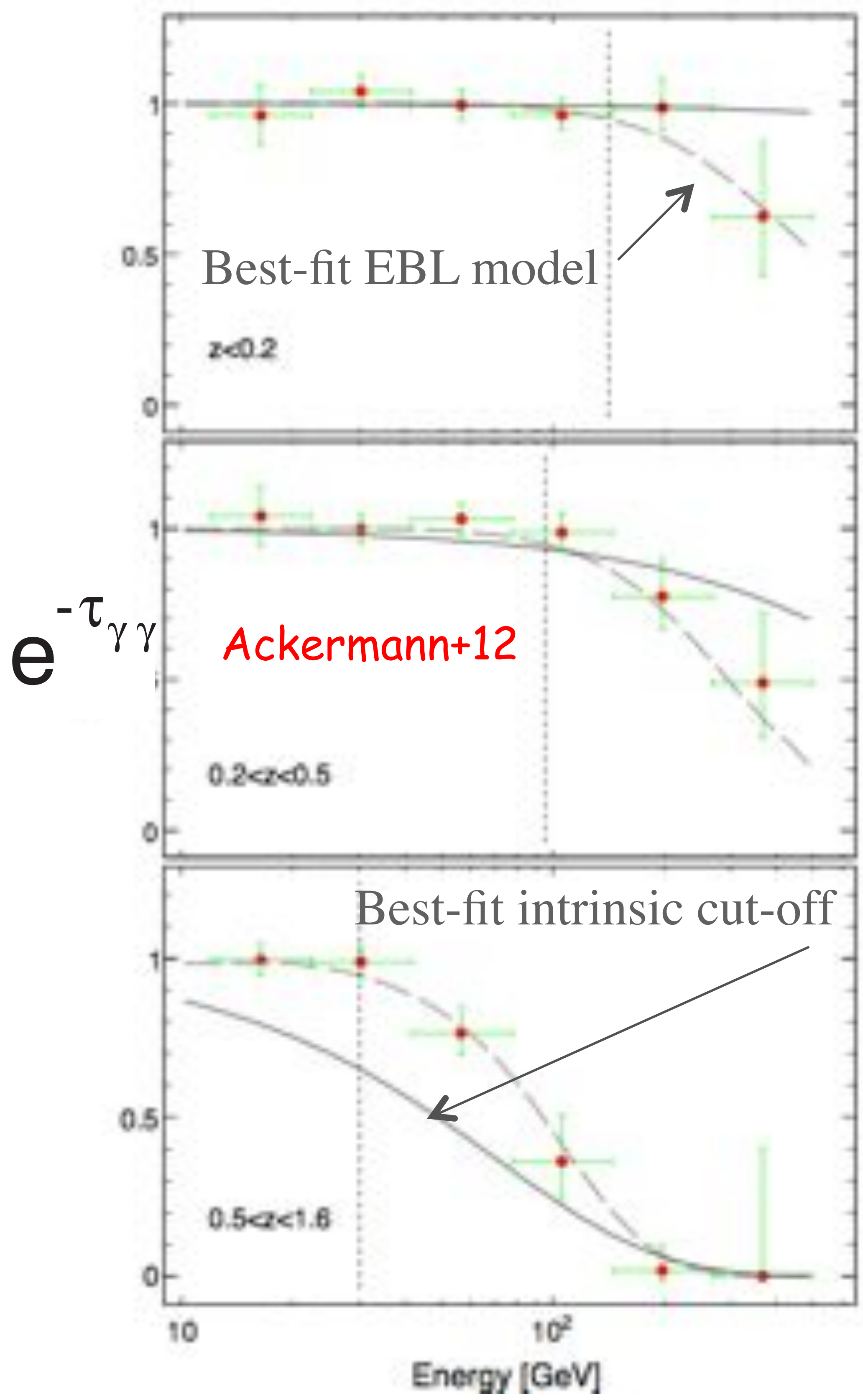

Best-fit EBL model

Ackermann+12

Best-fit intrinsic cut-off

M. Ackermann, M. Ajello, et al. (Fermi), Science 338, 1190 (2012)

Composite Likelihood Results

- A significant steepening in the blazars' spectra is detected
- This is consistent with that expected by a 'minimal' EBL:
  - i.e. EBL at the level of galaxy counts
  - 4 models rejected above 3sigma
- All the non-rejected models yield a significance of detection of 5.6-5.9 σ
- The level of EBL is 3-4 times lower than our previous UL (Abdo+10, ApJ 723, 1082)

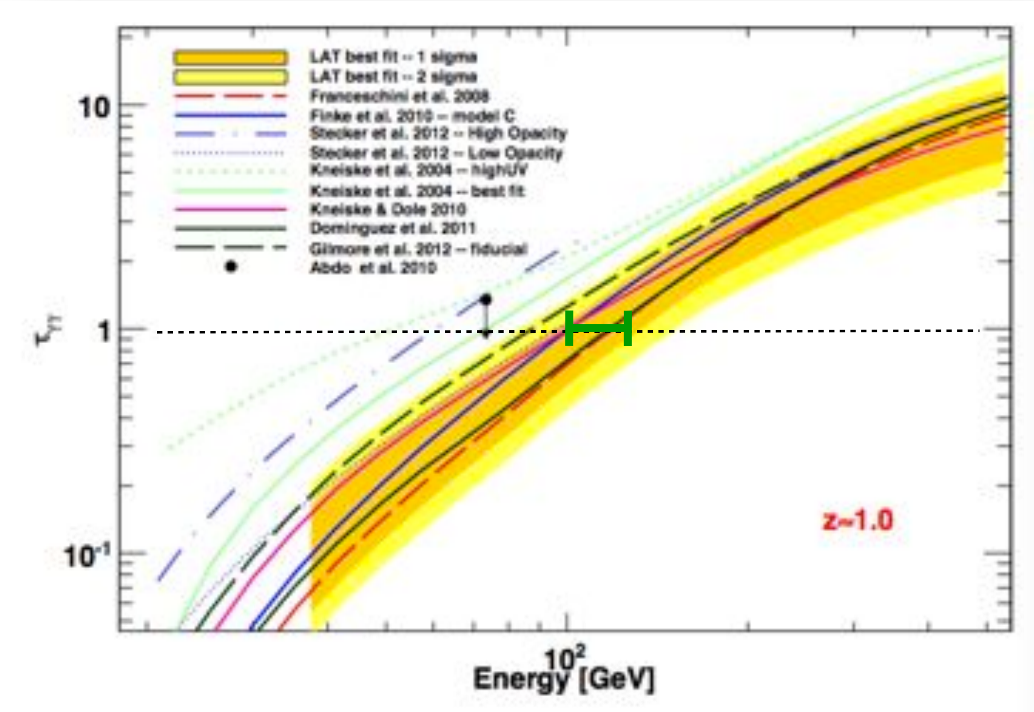

Ackermann+12

EBL Detection Significance

Model Rejection Significance

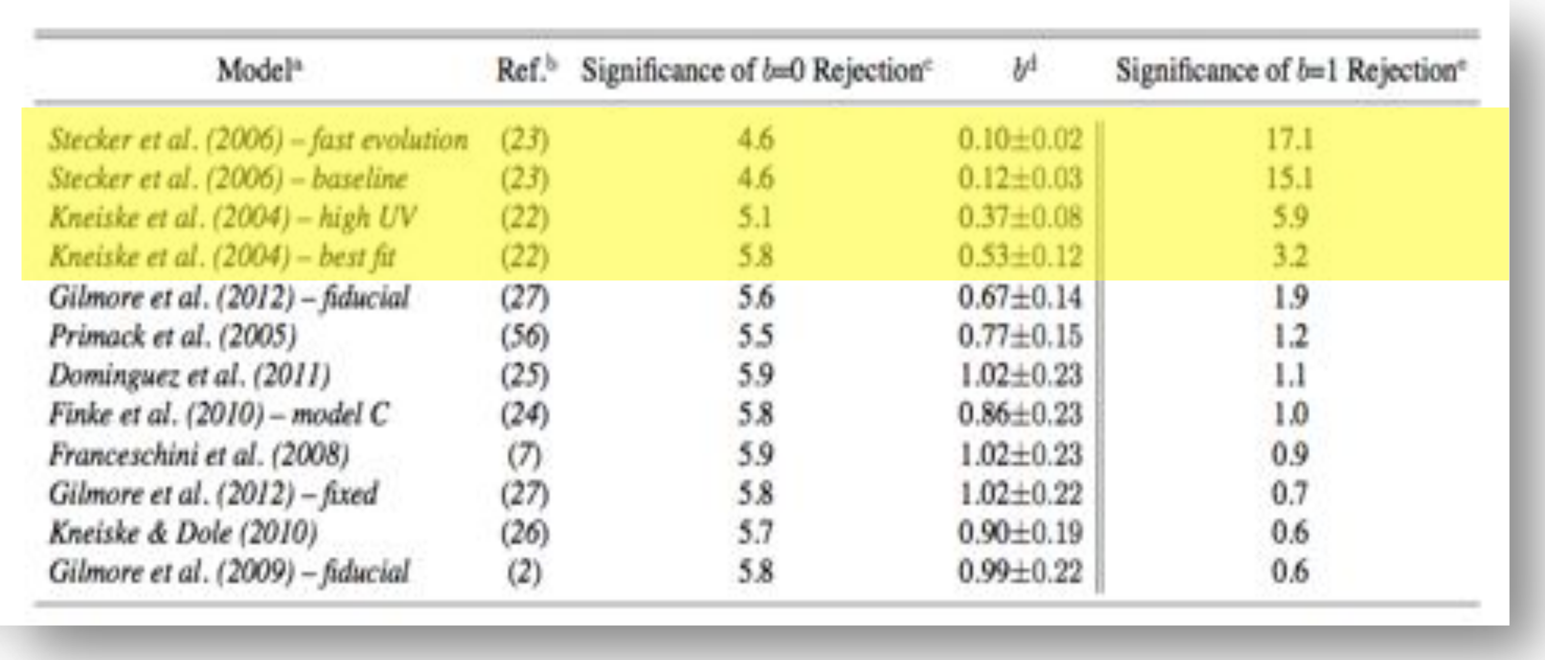

Model^a	Ref.^{b}	Significance of b=0 Rejection^c	b^d	Significance of b=1 Rejection^e
Stecker et al. (2006) – fast evolution	(23)	4.6	0.10±0.02	17.1
Stecker et al. (2006) – baseline	(23)	4.6	0.12±0.03	15.1
Kneiske et al. (2004) – high UV	(22)	5.1	0.37±0.08	5.9
Kneiske et al. (2004) – best fit	(22)	5.8	0.53±0.12	3.2
Gilmore et al. (2012) – fiducial	(27)	5.6	0.67±0.14	1.9
Primack et al. (2005)	(56)	5.5	0.77±0.15	1.2
Dominguez et al. (2011)	(25)	5.9	1.02±0.23	1.1
Finke et al. (2010) – model C	(24)	5.8	0.86±0.23	1.0
Franceschini et al. (2008)	(7)	5.9	1.02±0.23	0.9
Gilmore et al. (2012) – fixed	(27)	5.8	1.02±0.22	0.7
Kneiske & Dole (2010)	(26)	5.7	0.90±0.19	0.6
Gilmore et al. (2009) – fiducial	(2)	5.8	0.99±0.22	0.6

Cosmic Gamma-Ray Horizon Compared with EBL Models

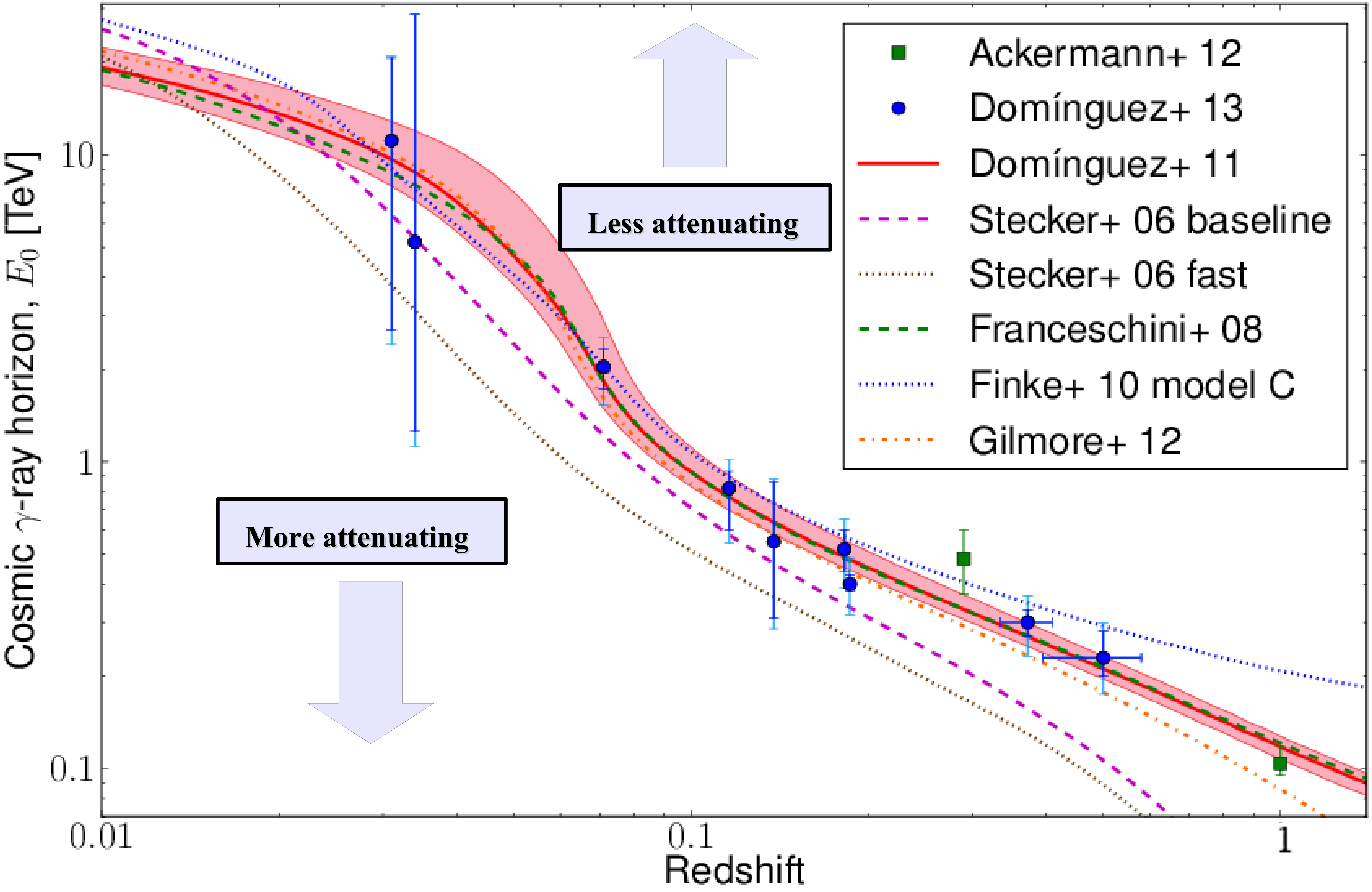

Monthly Notices of the ROYAL ASTRONOMICAL SOCIETY
420, 800–809 (2012)

Constraining the near-infrared background light from Population III stars using high-redshift gamma-ray sources

Rudy C. Gilmore

ABSTRACT The *Fermi* satellite has detected GeV emission from a number of gamma-ray bursts and active galactic nuclei at high redshift, $z \gtrsim 1.5$. We examine the constraints that the detections of gamma-rays from several of these sources place on the contribution of Population III stars to the extragalactic background light. Emission from these primordial stars, particularly redshifted Lyman α emission, can interact with gamma-rays to produce electron–positron pairs and create an optical depth to the propagation of gamma-ray emission, and the detection of emission at >10 GeV can therefore constrain the production of this background. We consider two initial mass functions for the early stars and use derived spectral energy distributions for each to put upper limits on the star formation rate density of massive early stars from redshifts 6 to 10. Our limits are complementary to those set on a high near-infrared background flux by ground-based TeV-scale observations and show that current data can limit star formation in the late stages of re-ionization to less than 0.5 $M_\odot$ yr^{-1} Mpc^{-3}. Our results also show that the total background flux from Population III stars must be considerably less than that from resolved galaxies at wavelengths below 1.5 μm.

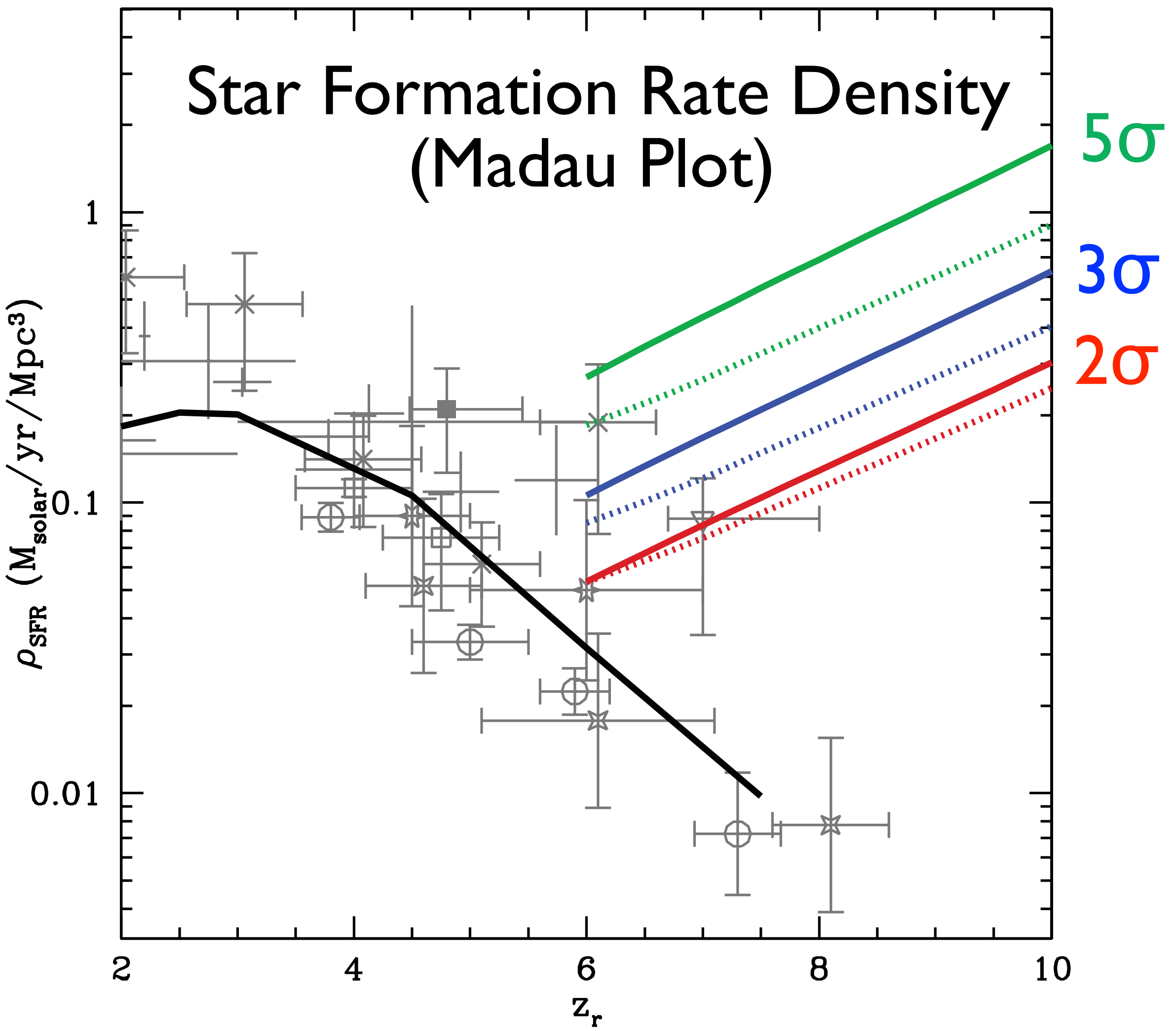

Upper bounds on the redshift z = 6 - 10 Pop-III SFRD in two possible scenarios with future *Fermi* GRBs, in the Larson IMF case. The solid lines show the limits from a GRB with the same redshift and spectral characteristics of GRB 080916C (z = 4.35), but with a highest energy observed photon of 30 GeV (160 GeV as emitted) instead of 13.2 GeV, in combination with the 5 most constraining $z \gtrsim 2$ sources (Abdo+2010). The dotted lines show a case with a GRB at z = 7 and a highest energy observed photon at 15 GeV (120 GeV emitted).

Conclusions

New data on attenuation of gamma rays from blazers

- X-ray + Fermi + ACT SSC fits to 9 blazars (Dominguez+12)
- Fermi data on 150 blazars at $z = 0 - 1.6$ (Ackermann+12)

now lead to statistically significant measurements of the cosmic gamma ray horizon and EBL as a function of source redshift and gamma ray energy.

These new measurements are consistent with recent EBL calculations based both on multiwavelength observations of thousands of galaxies and also on semi-analytic models of the evolving galaxy population. Such comparisons account for all the light, including that from galaxies too faint to see.

Catching a few high-redshift GRBs with Fermi or low-threshold atmospheric Cherenkov telescope arrays could provide important new constraints on the high-redshift star formation history of the universe.